vascular cast that remained was mounted on the stage of a scanning electron microscope (model S-3200 N; Hitachi, Tokyo, Japan) using colloidal silver paste, sputter-coated with osmium, and screened for arterial abnormalities.

Identified lesions were classified as shown in Fig. 1 based on the scanning electron microscopy findings as defined previously for arterial branching sites (Jamous et al., 2005a,b; Eldawoody et al., 2009). We were not able to randomize the rats for the post-surgical treatment using different drugs. Instead, we judged staging of aneurysmal lesions in a blinded fashion. Thus, the photos of the scanning electron microscope were prepared by the first author (N.K.). These photos were presented to two independent researchers (H.S., H.E) who were not informed about treatment. The two judged the staging of aneurysmal changes in a blinded fashion and if there was a difference between the judgments, the final decision was made by discussion between the two.

4.4. *Statistical analysis*

Despite the small numbers of samples, we used parametric statistics after confirming that most of the mean values of the parameters were more than 2 times larger than the corresponding standard deviations. Means of two independent groups were compared with Student's t-test. Means of more than three independent groups were compared with one way analysis of variance with Bonferroni's post-hoc test. Categorical data of aneurysm staging in each treated group were tested for statistical differences against Group C using the Chi-square test for trend. Statistical analyses were performed on a computer running statistical software (GraphPad Prism v.5; GraphPad Software Inc., La Jolla, CA). Differences were considered statistically significant when the probability value was less than 0.05.

Acknowledgments

We thank Drs. Michiaki Abe, Takafumi Toyohara, and Takaaki Abe (Division of Nephrology, Hypertension and Endocrinology, Department of Medicine, Tohoku University Graduate School of Medicine), for their valuable advice on the experimental hypertension model in rats. We also thank Daiichi-Sankyo Co. for kindly providing olmesartan and pravastatin.

REFERENCES

Aoki, T., Kataoka, H., Morimoto, M., Nozaki, K., Hashimoto, N., 2007a. Macrophage-derived matrix metalloproteinase-2 and -9 promote the progression of cerebral aneurysms in rats. Stroke 38, 162–169.

Aoki, T., Kataoka, H., Shimamura, M., Nakagami, H., Moriwaki, T., Ishibashi, R., Nozaki, K., Morishita, R., Hashimoto, N., 2007b. NF-kappa B is a key mediator of cerebral aneurysm formation. Circulation 116, 2830–2840.

Aoki, T., Kataoka, H., Ishibashi, R., Nozaki, K., Hashimoto, N., 2008. Simvastatin suppresses the progression of experimentally induced cerebral aneurysms in rats. Stroke 39, 1276–1285.

Aoki, T., Kataoka, H., Ishibashi, R., Nozaki, K., Egashira, K., Hashimoto, N., 2009a. Impact of monocyte chemoattractant protein-1 deficiency on cerebral aneurysm formation. Stroke 40, 942–951.

Aoki, T., Kataoka, H., Ishibashi, R., Nakagami, H., Nozaki, K., Morishita, R., Hashimoto, N., 2009b. Pitavastatin suppresses formation and progression of cerebral aneurysms through inhibition of the nuclear factor κB pathway. Neurosurgery 64, 357–366.

Aoki, T., Nishimura, M., Kataoka, H., Ishibashi, R., Nozaki, K., Hashimoto, N., 2009c. Reactive oxygen species modulate growth of cerebral aneurysms: a study using the free radical scavenger edaravone and p47phox(−/−) mice. Lab. Invest. 89, 730–741.

Aoki, T., Nishimura, M., Kataoka, H., Ishibashi, R., Miyake, T., Takagi, Y., Morishita, R., Hashimoto, N., 2009d. Role of angiotensin II type 1 receptor in cerebral aneurysm formation in rats. Int. J. Mol. Med. 24, 353–359.

Bruno, G., 1998. Vascular extracellular matrix remodeling in cerebral aneurysms. J. Neurosurg. 89, 431–440.

Cai, H., Harrison, D.G., 2000. Endothelial dysfunction in cardiovascular diseases: the role of oxidant stress. Circ. Res. 87, 840–844.

Chen, X.L., Tummala, P.E., Olbrych, M.T., Alexander, R.W., Medford, R.M., 1998. Angiotensin II induces monocyte chemoattractant protein-1 gene expression in rat vascular smooth muscle cells. Circ. Res. 83, 952–959.

Cruzan, G., 2009. Assessment of the cancer potential of methanol. Crit. Rev. Toxicol. 39, 347–363.

Davignon, J., 2004. Beneficial cardiovascular pleiotropic effects of statins. Circulation 109, 39–43.

De Keulenaer, G.W., Ushio-Fukai, M., Yin, Q., Chung, A.B., Lyons, P. R., Ishizaka, N., Rengarajan, K., Taylor, W.R., Alexander, R.W., Griendling, K.K., 2000. Convergence of redox-sensitive and mitogen-activated protein kinase signaling pathways in tumor necrosis factor-alpha-mediated monocyte chemoattractant protein-1 induction in vascular smooth muscle cells. Arterioscler. Thromb. Vasc. Biol. 20, 385–391.

Diet, F., Pratt, R.E., Berry, G.J., Momose, N., Gibbons, G.H., Dzau, V.J., 1996. Increased accumulation of tissue ACE in human atherosclerotic coronary artery disease. Circulation 94, 2756–2767.

Eldawoody, H., Shimizu, H., Kimura, N., Saito, A., Nakayama, T., Takahashi, A., Tominaga, T., 2009. Simplified experimental cerebral aneurysm model in rats: comprehensive evaluation of induced aneurysms and arterial changes in the circle of Willis. Brain Res. 1300, 159–168.

Fujiwara, Y., Shiraya, S., Miyake, T., Yamakawa, S., Aoki, M., Makino, H., Nishimura, M., Morishita, R., 2008. Inhibition of experimental abdominal aortic aneurysm in a rat model by the angiotensin receptor blocker valsartan. Int. J. Mol. Med. 22, 703–708.

Fukuda, S., Hashimoto, N., Naritomi, H., Nagata, I., Nozaki, K., Kondo, S., Kurino, M., Kikuchi, H., 2000. Prevention of rat cerebral aneurysm formation by inhibition of nitric oxide synthase. Circulation 101, 2532–2538.

Hashimoto, N., Handa, H., Nagata, I., Hazama, F., 1983. Saccular cerebral aneurysms in rats. Am. J. Pathol. 110, 397–399.

Hayashidani, S., Tsutsui, H., Shiomi, T., Suematsu, N., Kinugawa, S., Ide, T., Wen, J., Takeshita, A., 2002. Fluvastatin, a 3-hydroxy-3-methylglutaryl coenzyme a reductase inhibitor, attenuates left ventricular remodeling and failure after experimental myocardial infarction. Circulation 105, 868–873.

Hazama, F., Kataoka, H., Yamada, E., Kayembe, K., Hashimoto, N., Kojima, M., Kim, C., 1986. Early changes of experimentally induced cerebral aneurysms in rats. Light-microscopic study. Am. J. Pathol. 124, 399–404.

Hop, J.W., Rinkel, G.J., Algra, A., van Gijn, J., 1997. Case-fatality rates and functional outcome after subarachnoid hemorrhage. A systematic review. Stroke 28, 660–664.

Imanishi, T., Ikejima, H., Tsujioka, H., Kuroi, A., Kobayashi, K., Shiomi, M., Muragaki, Y., Mochizuki, S., Goto, M., Yoshida, K., Akasaka, T., 2008. Combined effects of an

3-hydroxy-3-methylglutaryl coenzyme A reductase inhibitor and angiotensin II receptor antagonist on nitric oxide bioavailability and atherosclerotic change in myocardial infarction-prone Watanabe heritable hyperlipidemic rabbits. Hypertens. Res. 31, 1199–1208.

Inagawa, T., 2001. Trends in incidence and case fatality rates of aneurysmal subarachnoid hemorrhage in Izumo City, Japan, between 1980–1989 and 1990–1998. Stroke 32, 1499–1507.

Ito, T., Yamakawa, H., Bregonzio, C., Term, J.A., Falcn-Neri, A., Saavedra, J.M., 2002. Protection against ischemia and improvement of cerebral blood flow in genetically hypertensive rats by chronic pretreatment with an angiotensin II AT1 antagonist. Stroke 33, 2297–2303.

Jamous, M.A., Nagahiro, S., Kitazato, K.T., Tamura, T., Aziz, H.A., Shono, M., Satoh, K., Satomi, J., 2005a. Role of estrogen deficiency in the formation and progression of cerebral aneurysms. Part I: experimental study of the effect of oophorectomy in rats. J. Neurosurg. 103, 1046–1051.

Jamous, M.A., Nagahiro, S., Kitazato, K.T., Tamura, T., Aziz, H.A., Shono, M., Satoh, K., Satomi, J., 2005b. Vascular corrosion casts mirroring early morphological changes that lead to the formation of saccular cerebral aneurysm: an experimental study in rats. J. Neurosurg. 102, 532–535.

Jamous, M.A., Nagahiro, S., Kitazato, K.T., Tamura, T., Aziz, H.A., Shono, M., Satoh, K., 2007. Endothelial injury and inflammatory response induced by hemodynamic changes preceding intracranial aneurysm formation: experimental study in rats. J. Neurosurg. 107, 410–411.

Koike, H., Sada, T., Mizuno, M., 2001. In vitro and in vivo pharmacology of olmesartan medoxomil, and angiotensin II type AT1 receptor antagonist. J. Hypertens. 19, S3–S14.

Kondo, S., Hashimoto, N., Kikuchi, H., Hazama, F., Nagata, I., Kataoka, H., 1998. Apoptosis of medial smooth muscle cells in the development of saccular cerebral aneurysms in rats. Stroke 29, 181–188.

Kubes, P., Suzuki, M., Granger, D.N., 1991. Nitric oxide: an endogenous modulator of leukocyte adhesion. Proc. Natl Acad. Sci. U. S. A. 88, 4651–4655.

Kumai, Y., Ooboshi, H., Ago, T., Ishikawa, E., Takada, J., Kamouchi, M., Kitazono, T., Ibayashi, S., Iida, M., 2008. Protective effects of angiotensin II type 1 receptor blocker on cerebral circulation independent of blood pressure. Exp. Neurol. 210, 441–448.

Linn, F.H., Rinkel, G.J., Algra, A., van Gijn, J., 1996. Incidence of subarachnoid hemorrhage: role of region, year, and rate of computed tomography: a meta-analysis. Stroke 27, 625–629.

Marui, N., Offermann, M.K., Swerlick, R., Kunsch, C., Rosen, C.A., Ahmad, M., Alexander, R.W., Medford, R.M., 1993. Vascular cell adhesion molecule-1 (VCAM-1) gene transcription and expression are regulated through an antioxidant-sensitive mechanism in human vascular endothelial cells. J. Clin. Invest. 92, 1866–1874.

Meng, H., Wang, Z., Hoi, Y., Gao, L., Metaxa, E., Swartz, D., Kolega, J., 2007. Complex hemodynamic at the apex of an arterial bifurcation induces vascular remodeling resembling cerebral aneurysm initiation. Stroke 38, 1924–1931.

Moriwaki, T., Takagi, Y., Sadamasa, N., Aoki, T., Nozaki, K., Hashimoto, N., 2006. Impaired progression of cerebral aneurysms in interleukin-1beta-deficient mice. Stroke 37, 900–905.

Nagata, I., 1979. Experimentally induced cerebral aneurysms in rats: part IV–cerebral angiography. Surg. Neurol. 12, 419–424.

Pahl, H.L., 1999. Activators and target genes of Rel/NF-kappaB transcription factors. Oncogene 18, 6853–6866.

Radomski, M.W., Palmer, R.M., Moncada, S., 1987. Endogenous nitric oxide inhibits human platelet adhesion to vascular endothelium. Lancet 7, 1057–1058.

Reidy, M.A., Levesque, M.J., 1977. A scanning electron microscopic study of arterial endothelial cells using vascular casts. Atherosclerosis 28, 463–470.

Ruiz-Ortega, M., 2001. Role of the renin–angiotensin system in vascular disease: expanding the field. Hypertension 38, 1382–1387.

Sadamasa, N., Nozaki, K., Hashimoto, N., 2003. Disruption of gene for inducible nitric oxide synthase reduces progression of cerebral aneurysms. Stroke 34, 2980–2984.

Stehbens, W.E., 1989. Etiology of intracranial berry aneurysms. J. Neurosurg. 70, 823–831.

Tada, Y., Kitazato, K.T., Tamura, T., Yagi, K., Shimada, K., Kinouchi, T., Satomi, J., Nagahiro, S., 2009. Role of mineralocorticoid receptor on experimental cerebral aneurysms in rats. Hypertension 54, 552–557.

Tamura, T., Jamous, M.A., Kitazato, K.T., Yagi, K., Tada, Y., Uno, M., Nagahiro, S., 2009. Endothelial damage due to impaired nitric oxide bioavailability triggers cerebral aneurysm formation in female rats. J. Hypertens. 27, 1284–1292.

Tummala, P.E., Chen, X.L., Sundell, C.L., Laursen, J.B., Hammes, C. P., Alexander, R.W., 1999. Angiotensin II induces vascular cell adhesion molecule-1 expression in rat vasculature: a potential link between the renin–angiotensin system and atherosclerosis. Circulation 100, 1223–1229.

van Gijn, J., Kerr, R.S., Rinkel, G.J., 2007. Subarachnoid haemorrhage. Lancet 27, 306–318.

Vasa, M., Fichtlscherer, S., Adler, K., Aicher, A., Martin, H., Zeiher, A.M., Dimmeler, S., 2001. Increase in circulating endothelial progenitor cells by statin therapy in patients with stable coronary artery disease. Circulation 103, 2885–2890.

Yamamoto, E., Yamashita, T., Tanaka, T., Kataoka, K., Tokutomi, Y., Lai, Z.F., Dong, Y.F., Matsuba, S., Ogawa, H., Kim-Mitsuyama, S., 2007. Pravastatin enhances beneficial effects of olmesartan on vascular injury of salt-sensitive hypertensive rats, via pleiotropic effects. Arterioscler. Thromb. Vasc. Biol. 27, 556–563.

Neuroscience Letters 470 (2010) 76–80

Contents lists available at ScienceDirect

Neuroscience Letters

journal homepage: www.elsevier.com/locate/neulet

Fasudil, a Rho-kinase inhibitor, attenuates induction and progression of cerebral aneurysms: Experimental study in rats using vascular corrosion casts

Hany Eldawoody[a,b,c,*], Hiroaki Shimizu[a,b], Naoto Kimura[a,b], Atsushi Saito[a], Toshio Nakayama[d], Akira Takahashi[b,d], Teiji Tominaga[a]

[a] Department of Neurosurgery, Tohoku University Graduate School of Medicine, Sendai, 980-8574, Japan
[b] Department of Neuroendovascular Therapy, Tohoku University Graduate School of Medicine, Sendai, Japan
[c] Department of Neurosurgery, Mansoura University, Mansoura, Egypt
[d] Department of Reconstructive Endovascular Therapy, Tohoku University Graduate School of Bio-medical Engineering, Sendai, Japan

ARTICLE INFO

Article history:
Received 24 September 2009
Received in revised form
26 November 2009
Accepted 22 December 2009

Keywords:
Cerebral aneurysm
Experimental
Fasudil
Rat

ABSTRACT

Fasudil (a Rho-kinase inhibitor) has been shown to attenuate abdominal aortic aneurysm development, but any preventive effect against development of cerebral aneurysms is unclear. The effect of fasudil on the development of cerebral aneurysms was investigated in 55 female Sprague-Dawley rats divided into 4 groups: Group 1 ($n = 10$) was the control group without treatment. Groups 2–4 ($n = 15$ each) were subjected to cerebral aneurysm induction procedures plus 1% NaCl in the drinking water. Groups 3 and 4 were also treated with 0.5 or 1.0 mg/mL of fasudil in the drinking water, respectively. Vascular corrosion casts of the cerebral arteries were prepared and examined using a scanning electron microscope after 2 months. No significant differences were observed in the degree of induced hypertension between Groups 2, 3 and 4. No aneurysms were found in Group 1. Examination of the left anterior cerebral–olfactory artery junction, which is the most susceptible site for aneurysm development, found significantly fewer aneurysmal lesions in Groups 3 (60%) and 4 (53%) compared to Group 2 (100%) ($P < 0.02$). This study suggests that fasudil attenuated induction of cerebral aneurysms in the rat model.

Cerebral aneurysm is a major cause of subarachnoid hemorrhage, which is fatal in approximately half of affected patients. The mechanisms of induction and growth of cerebral aneurysms have been investigated using various animal models of cerebral aneurysms including rats [10,16,17], mice [6], and monkeys [11]. Arterial hypertension is thought to be one of the major factors in the formation and rupture of saccular aneurysm [22]. Induced hypertension, by renal artery ligation, combined with carotid ligation has been used to enhance hemodynamic stress in the collateral pathway along the circle of Willis, finally resulting in aneurysmal changes [7,16,17,22].

Hemodynamic stress induces endothelial injury [10] which triggers macrophage infiltration [4] and proliferation and migration of the smooth muscle cells (SMCs) [17,25]. This results in the formation of an inflammatory zone at the apical intimal pad (AIP), possibly due to inflammatory cell-derived proteolytic enzymes. Subsequently, a defect in the inflammatory zone is created and the structural integrity of the vascular wall is disturbed. This defect, restricted to the area of migrated SMCs, represents the nidus of the intracranial aneurysm [17].

The Rho family consists of small guanosine triphosphate-binding proteins (G proteins) [25,26]. Rho-kinase has been widely studied as a main modulator of vascular SMCs through an intracellular calcium-independent pathway [8]. Rho-kinase also upregulates pro-inflammatory molecules [9,12] and downregulates endothelial nitric oxide synthase (eNOS) [28]. Fasudil is a Rho-kinase inhibitor, which suppresses inflammatory processes and consequently reduces endothelial dysfunction [1]. Deficiency of eNOS expression in the apical intimal pad in the arterial wall has been proposed as one of the early aneurysmal changes [17]. Fasudil may attenuate formation of abdominal aortic aneurysm through inhibition of both apoptosis and proteolysis pathways within the arterial wall [31]. However, whether fasudil has any effect on the development of cerebral aneurysms remains unknown.

This study investigated the potential beneficial effect of fasudil to inhibit the development of cerebral aneurysms.

The present experiments and protocols were conducted in accordance with the Japanese standards for the care and use of laboratory animals and were approved by the Animal Care Committee, Tohoku University Graduate School of Medicine. All surgical procedures were performed after induction of anesthesia.

* Corresponding author at: Department of Neurosurgery, Tohoku University Graduate School of Medicine, 1-1, Seiryo-machi, Aoba-ku, Sendai, 980-8574, Japan. Tel.: +81 22 717 7230; fax: +81 22 717 7233.
E-mail addresses: hanyeldawoody@yahoo.com, hanyeldawoody@ivns.med.tohoku.ac.jp (H. Eldawoody).

0304-3940/$ – see front matter © 2009 Elsevier Ireland Ltd. All rights reserved.
doi:10.1016/j.neulet.2009.12.061

Table 1
Experimental groups.

Group	Number of rats	Treatment		SABP at the end of experiment (mmHg, mean ± SEM)
		Surgery[a]	Post-surgical medication	
Group 1	10	–	–	125.3 ± 10.8
Group 2	15	+	1% NaCl in drinking water	181.1 ± 20.0[b]
Group 3	15	+	1% NaCl + fasudil 0.5 mg/mL in drinking water	180.5 ± 21.1[b]
Group 4	15	+	1% NaCl + fasudil 1.0 mg/mL in drinking water	180.1 ± 26.5[b]

SABP: systolic arterial blood pressure, SEM: standard error of the mean.
[a] Occlusion of posterior branches of bilateral renal arteries and right common carotid artery + bilateral oophorectomy.
[b] Statistically significant difference vs. Group 1 ($P < 0.01$, Dunn's multiple comparison test after one-way analysis of variance).

A total of 55 7-week-old female Sprague-Dawley rats (body weight 130–185 g) were divided into 4 groups (Table 1). Group 1 served as a control group without treatment to confirm the normal appearance of a vascular corrosion cast as described below. Groups 2–4 all underwent the following cerebral aneurysm induction procedure. After induction of anesthesia by intraperitoneal injection of pentobarbital (40 mg/kg, Nembutal; Dainippon Sumitomo Pharma Co., Ltd., Osaka, Japan), ligation of the right common carotid artery (CCA) and posterior branches of the bilateral renal arteries, and bilateral oophorectomy were performed. This rat model of experimental cerebral aneurysm was previously described [16], but we modified the surgical procedures to be performed at the same time [7]. On the same day of operation, 1% NaCl solution was provided as drinking water as an adjunct for induced renal hypertension. Groups 3 and 4 were also treated with fasudil powder (Asahi Kasei Corp., Tokyo, Japan) added to the drinking water at concentrations of 0.5 and 1.0 mg/mL, respectively.

Blood pressure was measured once a month in unanesthetized animals using the tail-cuff auto-pickup method (Softron Inc., Tokyo, Japan). Two months after the surgical procedure, all rats were euthanized and vascular corrosion casts of the cerebral arteries were prepared with the previously described method [7,16]. After induction of anesthesia, the rats underwent laparotomy and thoracotomy. The tip of a plastic cannula (18-Gauge caliber, length of 1.25 in.) was inserted into the left ventricle and secured in the ascending aorta with a superimposed ligature. After the right atrium was cut for drainage, the rats were perfused with 100 mL heparin/phosphate-buffered saline (20 U/mL) using a perfusion pump at 10 mL/min. This procedure was followed by manual injection of 10 mL Batson No. 17 plastic (Polysciences, Inc., Warrington, PA). After polymerization for 24 h at room temperature, the entire brain was removed and digested in 20% KOH for 24–72 h, with intermittent water rinses. The vascular cast that remained was mounted on the stage of a scanning electron microscope (model S-3200N; Hitachi, Tokyo, Japan) using colloidal silver paste, sputter-coated with osmium, and screened for arterial abnormalities with the scanning electron microscope.

This study investigated sites of increased hemodynamic stress in the collateral circulation after right CCA occlusion, specifically along the left internal carotid artery (ICA) to the left anterior cerebral artery (ACA), and along the basilar artery through the right posterior cerebral artery (PCA) and the right posterior communi-

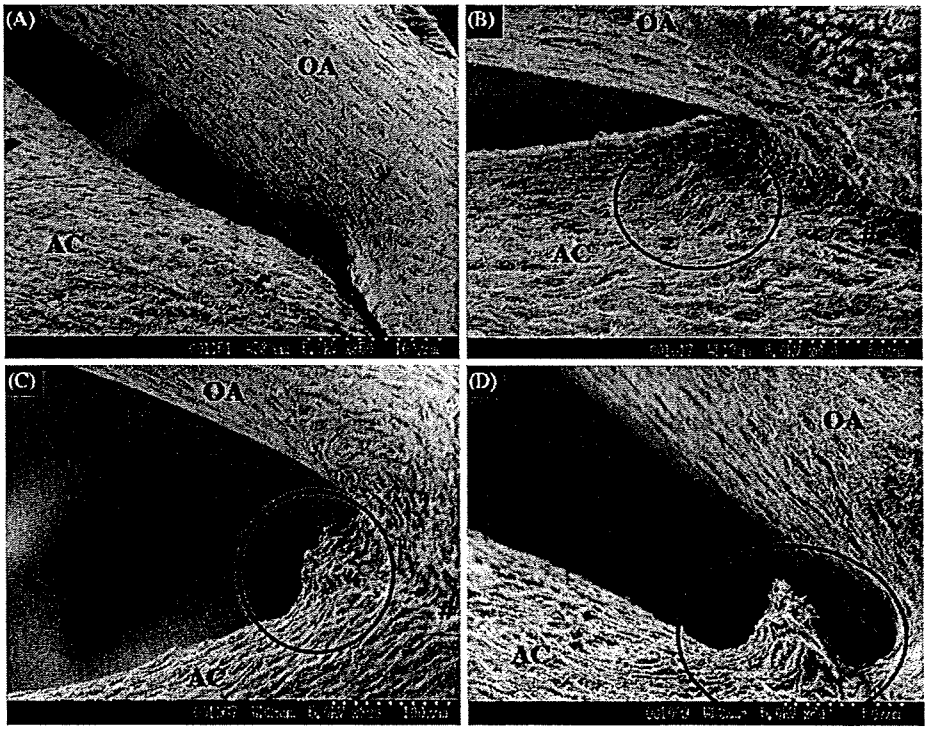

Fig. 1. Classification of aneurysmal changes at the branching sites based on the scanning electron microscopy findings. (A) Stage 0 (normal), normal endothelial cell imprints at the arterial bifurcation with no gross arterial dilatation compared to the contralateral side. (B) Stage I, roughened apical intimal pad with irregularly shaped imprints. (C) Stage II, shallow fusiform elevation at the apical intimal pad covered with abnormal imprints. (D) Stage III, saccular aneurysm covered with abnormal imprints. ACA: anterior cerebral artery, OA: olfactory artery, #: non-pathological cleft found in all corrosion casts between ACA and OA.

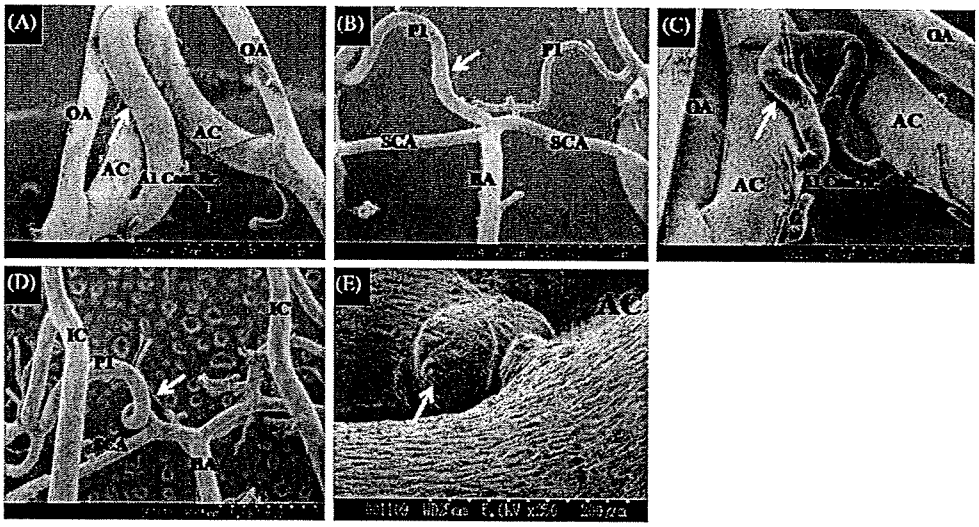

Fig. 2. Classification of aneurysmal changes at non-branching sites. (A) Dilatation of the A1 communicating branch (arrow). Maximum diameter greater than that of the left olfactory artery was considered to indicate dilatation. (B) Dilatation of the right P1 segment (arrow). Uniform or multiple dilatations of the artery along the longitudinal direction with maximum diameter ≥1.5 times that of the contralateral corresponding artery was considered to indicate dilatation. (C) Tortuosity of the A1 communicating branch. Tortuosity was indicated by a hair pin-like curve due to presumed longitudinal elongation. (D) Tortuosity of the right P1 (looping, arrow). At least 3 sharp curvatures (<45°) or a minimum of one loop was considered to indicate tortuosity. (E) Fusiform aneurysm seen at the fenestration of the A1 (arrow). Focal, segmental, and circumscribed dilatation involving an entire vessel wall ≥1.5 times the diameter of the normal portion or the diameters at both ends.

cating artery (PcoA) to the right ICA. In the rat, the bilateral proximal parts of the ACA (A1) form the azygos artery before separation into the bilateral distal ACAs, and there is no obvious anterior communicating artery (AcoA) [19]. The relatively large olfactory artery (OA) arises from the A1 before merging into the azygos artery. The A1 is also characterized by frequent formation of fenestrations. The main flow into the PCA comes from the ICA through the PcoA, and the P1 that originates from the basilar terminal portion is relatively smaller than the PcoA. Previous studies of experimental cerebral aneurysms have described aneurysms of the AcoA in rats [17,22], and we actually found one or more fine branches connecting both A1s in control rats and a dilated branch mimicking the AcoA in experimental rats [7], so we tentatively referred to these fine branches as the A1 communicating branches. Any identified lesions were classified based on our preliminary findings [7] (Figs. 1 and 2). The judgment of aneurysmal changes (number and staging) in each rat was carried out by two independent researchers (H.S., N.K.) based on photos of the scanning electron microscope taken by the first author (H.E.). The two referees were blinded for the treatment. If there was a difference in the judgment, the final decision was made through a discussion between the two.

Differences between more than three independent groups were compared by one-way analysis of variance with Dunnett's post-hoc test. Categorical data between groups were tested for differences using the Chi-square test or Fisher's exact test. Statistical analyses used statistical software (GraphPad Prism v5, San Diego, CA). Differences were considered statistically significant if the probability value was less than 0.05.

Groups 2–4 showed significant increases in systolic arterial blood pressure at the end of the experiment compared with Group 1 (Table 1).

Group 1 showed no aneurysmal lesions at branching or non-branching sites. The clefts in Fig. 1 (marked by #) were judged to be non-pathological findings or artifacts, because such findings were also evident among all rats in Group 1.

A total of 53 lesions were detected at branching sites (Table 2). Groups 3 contained significantly fewer induced aneurysmal lesions compared with Group 2 ($P < 0.05$). Group 4 showed a similar but not statistically significant tendency. Analysis of the left ACA-OA bifurcation, the most susceptible site for aneurysm development, found significantly fewer aneurysmal lesions in Groups 3 ($P = 0.017$) and 4 ($P = 0.006$) compared with Group 2. The staging pattern of aneurysmal lesions at this site tended to be different between groups ($P = 0.06$), but if stage 0 was excluded from the analysis pattern, stages 1–3 were similar in all groups ($P = 0.56$).

Non-branching sites with increased hemodynamic stress in the collateral circulation after right CCA ligation were also investigated for possible abnormal lesions (Fig. 2, Table 3). However, lesions were confined to the A1 communicating branches and the right P1 segment. A total of 80 lesions were detected with no significant

Table 2
Branching site lesions.

	Group 2	Group 3	Group 4
Number of rats	15	15	15
Total number of lesions	24	13	16
Number of lesions per rat (mean ± SEM)*	1.6 ± 0.2	0.9 ± 0.2	1.1 ± 0.3
Site			
No lesion	0 (0%)	5 (33%)	6 (40%)
Left ACA-OA	15 (100%)	9 (60%)**	8 (53%)**
Left A1 (fenestration or its branch)	6 (40%)	2 (13%)	2 (13%)
Left ICA bifurcation	2 (13%)	2 (13%)	4 (27%)
Right PCA	1 (7%)	0	2 (13%)
Staging of left ACA-OA lesions***			
Stage 0	0 (0%)	6 (40%)	7 (47%)
Stage 1	3 (20%)	0 (0%)	2 (13%)
Stage 2	8 (53%)	6 (40%)	5(33%)
Stage 3	4 (27%)	3 (20%)	1 (7%)

Percentages indicate incidence of lesions per rat.
SEM: standard error of the mean; ACA: anterior cerebral artery; OA: olfactory artery; ICA: internal carotid artery; PCA: posterior cerebral artery.
* Difference in number of lesions per rat is statistically significant between the 3 groups ($P = 0.0499$). Post-hoc Dunn's test reveals significant difference only between Groups 2 and 3.
** Incidences of aneurysmal lesion in Groups 3 and 4 are significantly different from that of Group 2 ($P = 0.017$ and 0.006, respectively, by Fisher's exact test).
*** See text for staging description. Staging pattern of 3 groups tends to be different but did not reach statistical significance ($P = 0.06$). When stage 0 is excluded, staging pattern of 3 groups is statistically similar ($P = 0.56$).

Table 3
Non-branching site lesions.

	Group 2	Group 3	Group 4
Number of rats	15	15	15
Total number of lesions	22	30	28
Number of lesions per rat (mean ± SEM)	1.3 ± 0.3	1.9 ± 0.2	1.9 ± 0.3
Site			
A1 communicating branch			
Fusiform	0	3	1
Dilatation	3	4	4
Tortuosity	1	2	2
Right P1			
Fusiform	0	0	0
Dilatation	13	13	13
Tortuosity	5	8	8

SEM: standard error of the mean.

differences between the groups. Lesion types (dilatation, tortuosity, fusiform and lateral wall aneurysms) were also not significantly different between the groups.

There is a controversy about the effect of fasudil on arterial blood pressure; while Uehata et al. [29] and Mukai et al. [21] demonstrated a blood pressure lowering effect, others observed no effect [13,31]. Our data also showed no effect on the blood pressure at the end of experiment. The reasons of these discrepancies may be due to dose and method of administration, timing of blood pressure measurement, difference in animals or species used in each experiment.

The present findings suggest that fasudil attenuated the induction of aneurysmal lesions at branching sites as shown in Table 2. Fasudil may not have markedly influenced aneurysm progression because the staging patterns showed no differences between the groups with or without fasudil. Further study will be necessary to identify the factors related to initiation and progression of aneurysm development.

In this study, we did not measure the serum fasudil concentration in each rat; however, a previous study using a similar administration method in the drinking water [31] suggests that a daily dose of 213 ± 10 mg/kg corresponds a plasma fasudil level of 0.7 ± 0.4 μmol/L. This plasma fasudil level may correlate with our high dose fasudil group (same dosage used, 1.0 mg/mL). Although the relatively large standard deviation may imply variation in doses of actual intake by each animal. When mice were given 100 mg/kg/day fasudil orally, the plasma concentration of hydroxyl fasudil was 0.37 ± 0.12 μmol/L [15].

The effect of fasudil on non-branching site lesions was not evident as shown in Table 3. Non-branching site lesions in the rat model of cerebral aneurysms have been investigated in only one study [18]. We found that fasudil significantly decreased the number of branching site lesions but not the number of non-branching site lesions, suggesting that different development mechanisms may be responsible for the two types of lesions, which also requires further study.

The vascular endothelial layer has been considered to be an indispensable autocrine and paracrine organ in the maintenance of vascular homeostasis by secreting various relaxing factors as prostacyclin, nitric oxide, and endothelial derived hyper polarizing factor (EDHF) [27]. It has been stated that H_2O_2 is the EDHF [20,27], whereas the major source of EDHF/H_2O_2 is eNOS [20].

Primary endothelial injury at the AIP of the arterial bifurcation, characterized by loss of eNOS expression [17], is thought to be induced by hemodynamic stresses that could be augmented by hypertension [10]. Angiotensin II increases oxidative stresses [9] by production of reactive oxygen species (ROS) through activation of nicotinamide adenine dinucleotide phosphate (NADPH) oxidases [23] and matrix metalloproteinases (MMPs) [5]. As a result, the highly expressed cyclophilin A (CypA) in VSMCs promotes activation of MMP-2 and synergistically augments ROS generation leading to vascular inflammation [24]. Vascular inflammation is enhanced by monocyte and macrophage infiltration guided by chemoattractant factors such as monocyte chemoattractant protein and macrophage migration inhibitory factor [4,17]. Recruited macrophages secrete proteolytic enzymes (cathepsins B, K, S [3], MMP 2, 9 [4]) and proapoptotic factors [31] that finally cause thinning of the medial SMC layer through degradation of the extracellular matrix, and apoptosis and/or migration of SMCs. Therefore, any intervention which reduces the inflammatory processes may prevent aneurysmal development [2–4].

Activation of Rho-kinase enhances atherosclerotic processes as it causes vascular SMC hypercontractility [8], stimulates vascular SMC proliferation and migration, inhibits vascular SMC apoptosis [8], downregulates Kruppel-like factor 2 (KLF2)/eNOS system [28,30], and enhances accumulation of inflammatory cells [13,31] through upregulation of some pro-inflammatory molecules [9,12]. Angiotensin II significantly increases Rho-kinase activity in vivo, which can be inhibited by treatment with fasudil [13]. Fasudil ameliorates endothelial dysfunction through normalization of the endothelial production of superoxide anions [13], suppresses vascular SMC migration, macrophage infiltration [2] and upregulates eNOS expression [25]. Fasudil also inhibits CypA secretion from VSMCs with subsequent down regulation of both ROS and MMP activities [24]. If aneurysmal change originates from the pathological imbalance between constructive and destructive processes within the arterial wall, all these effects of fasudil could be beneficial for attenuating aneurysm induction.

Rho-kinase upregulation by inflammatory stimuli (e.g. angiotensin II and IL-1β) which is mediated by protein kinase C and NF-κB pathways [14] downregulates eNOS [28]. Estrogen exerts an inhibitory modulation on Rho-kinase through protein kinase C/NF-κB pathways resulting in upregulation of eNOS [15]. Oophorectomy induced estrogen deficiency in our experiment releases Rho-kinase from the estrogen inhibitory effect. Fasudil, being a rho-kinase inhibitor, may partially reverse this initiation mechanism involved in aneurysm formation.

The main observation of this study was that fasudil attenuated the formation of aneurysmal lesions at arterial branching sites. No dose-dependency was observed in the present settings, and no effect was seen at non-branching sites. This study was designed as a preliminary step in the investigation of the novel effects of fasudil on cerebral aneurysm development. Further study is required to clarify the dose-dependency of fasudil, the related changes to fasudil in various biological markers and on which pathways of aneurysm initiation and/or progression fasudil exerts its protective effect.

Acknowledgments

We thank Professor Hiroaki Shimokawa and Dr. Shunsuke Tawara (Department of Cardiovascular Medicine, Tohoku University Graduate School of Medicine) for their valuable advice on the use of the fasudil in rats. We also thank Asahi Kasei Corp. (Tokyo, Japan) for generously providing us fasudil powder.

References

[1] K. Abe, H. Shimokawa, K. Morikawa, T. Uwatoku, K. Oi, Y. Matsumoto, T. Hattori, Y. Nakashima, K. Kaibuchi, K. Sueishi, A. Takeshita, Long-term treatment with a Rho-kinase inhibitor improves monocrotaline-induced fatal pulmonary hypertension in rats, Circ. Res. 94 (2004) 385–393.
[2] T. Aoki, H. Kataoka, M. Morimoto, K. Nozaki, N. Hashimoto, Macrophage derived matrix metalloproteinase-2 and -9 promote the progression of cerebral aneurysms in rats, Stroke 38 (2007) 162–169.

[3] T. Aoki, H. Kataoka, R. Ishibashi, K. Nozaki, N. Hashimoto, Cathepsin B, K, and S are expressed in cerebral aneurysms and promote the progression of cerebral aneurysms, Stroke 39 (2008) 2603–2610.
[4] T. Aoki, H. Kataoka, R. Ishibashi, K. Nozaki, K. Egashira, N. Hashimoto, Impact of monocyte chemoattractant protein-1 deficiency on cerebral aneurysm formation, Stroke 40 (3) (2009) 942–951.
[5] M. Browatzki, D. Larsen, C.A. Pfeiffer, S.G. Gehrke, J. Schmidt, A. Kranzhofer, H.A. Katus, R. Kranzhofer, Angiotensin II stimulates matrix metalloproteinase secretion in human vascular smooth muscle cells via nuclear factor-kB and activator protein 1 in a redox-sensitive manner, J. Vasc. Res. 42 (2005) 415–423.
[6] M. Coutard, Experimental cerebral aneurysms in the female heterozygous Blotchy mouse, Int. J. Exp. Path. 80 (1999) 357–367.
[7] H. Eldawoody, H. Shimizu, N. Kimura, A. Saito, T. Nakayama, A. Takahashi, T. Tominaga, Simplified experimental cerebral aneurysm model in rats: comprehensive evaluation of induced aneurysms and arterial changes in the circle of Willis, Brain Res. 1300 (2009) 159–168.
[8] Y. Fukata, M. Amano, K. Kaibuchi, Rho-Rho-kinase pathway in smooth muscle contraction and cytoskeletal reorganization of non-muscle cells, Trends Pharmacol. Sci. 22 (2001) 32–39.
[9] Y. Funakoshi, T. Ichiki, H. Shimokawa, K. Egashira, K. Takeda, K. Kaibuchi, M. Takeya, T. Yoshimura, A. Takeshita, Rho-kinase mediates angiotensin II-induced monocyte chemoattractant protein-1 expression in rat vascular smooth muscle cells, Hypertension 38 (2001) 100–104.
[10] N. Hashimoto, H. Handa, I. Nagata, F. Hazama, Experimentally induced cerebral aneurysms in rats: Part V, Relation of hemodynamics in the circle of Willis to formation of aneurysms, Surg. Neurol. 13 (1980) 41–45.
[11] N. Hashimoto, C. Kim, H. Kikuchi, M. Kojima, Y. Kang, F. Hazama, Experimental induction of cerebral aneurysms in monkeys, J. Neurosurg. 67 (1987) 903–905.
[12] T. Hattori, H. Shimokawa, M. Higashi, J. Hiroki, Y. Mukai, H. Tsutsui, A. Kaibuchi, Takeshita, Long-term inhibition of Rho-kinase suppresses left ventricular remodeling after myocardial infarction in mice, Circulation 109 (2004) 2234–2239.
[13] M. Higashi, H. Shimokawa, T. Hattori, J. Hiroki, Y. Mukai, K. Morikawa, T. Ichiki, S. Takahashi, A. Takeshita, Long-term inhibition of Rho-kinase suppresses angiotensin II-induced cardiovascular hypertrophy in rats in vivo. Effects on endothelial NAD(P)H oxidase system, Circ. Res. 93 (2003) 767–775.
[14] J. Hiroki, H. Shimokawa, M. Higashi, K. Morikawa, T. Kandabashi, N. Kawamura, T. Kubota, T. Ichiki, A. Mutsuki, K. Kaibuchi, A. Takeshita, Inflammatory stimuli upregulate Rho-kinase in human coronary vascular smooth muscle cells, J. Mol. Cell. Cardiol. 37 (2004) 537–546.
[15] J. Hiroki, H. Shimokawa, Y. Mukai, T. Ichiki, A. Takeshita, Divergent effects of estrogen and nicotine on Rho-kinase expression in human coronary vascular smooth muscle cells, Biophys. Biochem. Res. Commun. 159 (26) (2005) 154.
[16] M.A. Jamous, S. Nagahiro, K.T. Kitazato, J. Satomi, Role of estrogen deficiency in the formation and progression of cerebral aneurysms. Part I: experimental study of the effect of oophorectomy in rats, J. Neurosurg. 103 (2005) 1046–1051.
[17] M.A. Jamous, S. Nagahiro, K.T. Kitazato, T. Tamura, H. Abdel aziz, M. Shono, K. Satoh, Endothelial injury and inflammatory response induced by hemodynamic changes preceding intracranial aneurysm formation: experimental study in rats, J. Neurosurg. 107 (2007) 405–411.
[18] S. Kondo, N. Hashimoto, H. Kikuchi, F. Hazama, I. Nagata, H. Kataoka, Cerebral aneurysms arising at nonbranching sites—an experimental study, Stroke 28 (1997) 398–404.
[19] R.M. Lee, Morphology of cerebral arteries, Pharmacol. Ther. 66 (1995) 149–173.
[20] T. Matoba, H. Shimokawa, M. Nakashima, Y. Hirakawa, Y. Mukai, K. Hirano, H. Kanaide, A. Takeshita, Hydrogen peroxide is an endothelium-derived hyperpolarizing factor in mice, J. Clin. Invest. 106 (2000) 1521–1530.
[21] Y. Mukai, H. Shimokawa, T. Matoba, T. Kandabashi, S. Satoh, K. Kaibuchi, A. Takeshita, Involvement of Rho-kinase in hypertensive vascular disease. A novel therapeutic target in hypertension, FASEB J. 15 (2001) 1062–1064.
[22] I. Nagata, H. Handa, N. Hashimoto, F. Hazama, Experimentally induced cerebral aneurysms in rats: VI. Hypertension, Surg. Neurol. 14 (1980) 477–479.
[23] S. Rajagopalan, S. Kurz, T. Münzel, M. Tarpey, B.A. Freeman, K.K. Griendling, D.G. Harrison, Angiotensin II-mediated hypertension in the rat increases vascular superoxide production via membrane NADH/NADPH oxidase activation. Contribution to alterations of vasomotor tone, J. Clin. Invest. 97 (1996) 1916–1923.
[24] K. Satoh, P. Nigro, T. Matoba, M.R. O'Dell, Z. Cui, X. Shi, A. Mohan, C. Yan, J. Abe, K.A. Illig, B.C. Berk, Cyclophilin A enhances vascular oxidative stress and the development of angiotensin II-induced aortic aneurysms, Nat. Med. 15 (2009) 649–656.
[25] H. Shimokawa, A. Takeshita, Rho-kinase is an important therapeutic target in cardiovascular medicine, Arterioscler. Thromb. Vasc. Biol. 25 (2005) 1767–1775.
[26] Y. Takai, T. Sasaki, T. Matozaki, Small GTP-binding proteins, Physiol. Rev. 81 (2001) 153–208.
[27] A. Takaki, K. Morikawa, Y. Murayama, E. Tekes, H. Yamagishi, J. Ohashi, M. Tsutsui, T. Yada, N. Yanagihara, H. Shimokawa, Crucial role of nitric oxide synthases system in endothelium-dependent hyperpolarization in mice, J. Exp. Med. 205 (9) (2008) 2053–2063.
[28] M. Takemoto, J. Sun, J. Hiroki, H. Shimokawa, J.K. Liao, Rho-kinase mediates hypoxia-induced downregulation of endothelial nitric oxide synthase, Circulation 106 (2002) 57–62.
[29] M. Uehata, T. Ishizaki, H. Satoh, T. Ono, T. Kawahara, T. Morishita, H. Tamakawa, K. Yamagami, J. Inui, M. Maekawa, S. Narumiya, Calcium sensitization of smooth muscle mediated by a Rho-associated protein kinase in hypertension, Nature 389 (1997) 990–994.
[30] J.V. van Thienen, J.O. Fledderus, R.J. Dekker, J. Rohlena, G.A. van Ijzendoorn, N.A. Kootstra, H. Pannekoek, A.J. Horrevoets, Shear stress sustains atheroprotective endothelial KLF2 expression more potently than statins through mRNA stabilization, Cardiovasc. Res. 72 (2006) 231–240.
[31] Y.X. Wang, B. Martin-McNulty, V.d. Cunha, J. Vincelette, X. Lu, Q. Feng, M. Halks-Miller, M. Mahmoudi, M. Schroeder, B. Subramanyam, J.L. Tseng, G.D. Deng, S. Schirm, A. Johns, K. Kauser, W.P. Dole, D.R. Light, Fasudil, a Rho-kinase inhibitor, attenuates angiotensin II-induced abdominal aortic aneurysm in apolipoprotein-deficient mice by inhibiting apoptosis and proteolysis, Circulation 111 (2005) 2219–2226.

Bacterial population moves toward a colon-like community in the pouch after total proctocolectomy

Atsushi Kohyama, MD,[a] Hitoshi Ogawa, MD,[a] Yuji Funayama, MD,[d] Ken-ichi Takahashi, MD,[d] Yoshimi Benno, DVM, PhD,[e] Katsunori Nagasawa, PhD,[f] Shin-ichi Tomita, PhD,[f] Iwao Sasaki, MD, FACS,[a] *and* Kouhei Fukushima, MD,[b,c] *Sendai, Saitama, and Tokyo, Japan*

Background. *Colonic transformation is defined by phenotypic alterations in the ileum after total proctocolectomy. Changes in microbiota of the ileal pouch and the roles of these microbes in colonic transformation, however, have not been addressed.*

Methods. *A total of 151 stool samples were collected from patients with ulcerative colitis patients and an ileostomy, those with an ileal pouch, and healthy control volunteers. Bacterial DNA was extracted from stool, and the diversity of complex bacteria was assessed by terminal restriction fragment length polymorphism (T-RFLP) analysis, a novel DNA-based approach that enables us to investigate the presence of nonculturable bacteria. To determine whether ileal pouch bacterial communities shift to a more colon-like distribution, the relative abundance of terminal restriction fragments that could be classified as "colonic," "ileal," or "common" was investigated.*

Results. *Cluster analysis demonstrated that most of the ileostomy samples were categorized into Cluster I or II and that less than 10% of ileostomy samples were classified into Cluster IV. In contrast, more than 90% of control samples were grouped in Cluster IV. In further analyses, the median lifetimes of pouches in Clusters I, II, III, and IV were significantly different at 11, 56, 265, and 310 days, respectively. T-RFLP patterns of the ileal pouch were characterized by a time-dependent decrease in "ileal" and increase in a part of "colonic" fragments, which represented mainly nonculturable bacteria such as the Clostridium coccoides group.*

Conclusion. *T-RFLP analysis demonstrated that a time-dependent shift to a "colon-like" bacterial community, including nonculturable bacteria, in the ileal pouch after total proctocolectomy. (Surgery 2009;145:435-47.)*

From the Division of Biological Regulation and Oncology, Department of Surgery,[a] and the Division of Molecular and Surgical Pathophysiology,[b] Tohoku University, Graduate School of Medicine, Sendai; Laboratory of Gastrointestinal Tract Reconstruction, Department of Regenerative Medicine, Tohoku University, Graduate School of Biomedical Engineering,[c] Sendai; Tohoku Rosai Hospital,[d] Sendai; Microbe Division/Japan Collection of Microorganisms, RIKEN BioResource Centre, Wako,[e] Saitama; and Department of Agricultural Chemistry, Tamagawa University,[f] Tokyo, Japan

TOTAL PROCTOCOLECTOMY (TPC) followed by ileal pouch-anal anastomosis (IPAA) is an established surgical treatment for ulcerative colitis (UC) and familial adenomatous polyposis (FAP).[1] After removal of the entire colon, patients are cured of disease without receiving a permanent ileostomy. Postoperative adaptive changes in the intestine, termed "intestinal adaptations," are thought to be advantageous for maintaining homeostasis. Microarray data derived from isolated epithelial cells show that intestinal adaptation is characterized, at least in part, by a colon-like transformation of ileal epithelia (ie, ileal epithelial cells assume a partial colonic phenotype and lose characteristics of the ileal phenotype).[2] Changes include an enhancement of water and electrolyte absorption in the remnant small intestine over time, which improves stool consistency from a watery diarrhea to paste stool.

The human gastrointestinal tract harbors a complex community of more than 10^{14} microorganisms, which is 10 times the total number of cells within the body.[3] Bacteria comprise approximately 55% of fecal solids. The metabolic activity of human gut microbiota is equivalent to that of any organ in the human body. Gut flora also affect host

Accepted for publication December 15, 2008.

Reprint requests: Kouhei Fukushima, MD, Laboratory of Gastrointestinal Tract Reconstruction, Department of Regenerative Medicine, Tohoku University, Graduate School of Biomedical Engineering, Seiryo-machi, Aoba-ku, Sendai 980-8574, Japan. E-mail: kouhei@surg1.med.tohoku.ac.jp.

0039-6060/$ - see front matter

doi:10.1016/j.surg.2008.12.003

Table I. Summary of samples

	Ileostomy	*Pouch after IC (<2 years)*	*Pouch after IC (>2 years)*	*Control*
Total no. of samples	34	73	13	31
No. of patients (male:female)	13 (7:6)	26 (16:9)	11 (7:4)	31 (31:0)
Age, y (range)	29 (22–66)	30 (17–62)	38 (23–32)	22 (20–32)
No. of patients with steroids	12 (31)*	0 (0)*	0 (0)*	0 (0)*
No. of patients with probiotics	4 (7)*	3 (8)*	2 (2)*	0 (0)*
No. of patients with antibiotics	11 (11)*	0 (0)*	0 (0)*	0 (0)*

IC, Ileostomy closure.
*No. of samples.

immunity and may be an important contributor to immune responses in later life. This community of mostly anaerobic bacteria influences human gut physiology and health through a number of activities, including fermentation of dietary components, production of short-chain fatty acids, modulation of the immune system, transformation of bile acids, production of vitamins and other health-protective substances, and provision of a barrier against pathogenic bacteria.[4] In fact, enteric bacteria modulate epithelial gene expression substantially.[5,6] For these reasons, we hypothesized that changes in the number and/or type of enteric microbiota are intimately associated with the adaptation process after TPC. To test this hypothesis, we investigated changes in enteric microbe communities that occur in a time-dependent fashion after TPC, as do changes in epithelial cell phenotype.

Traditional methods for determining the composition of intestinal microbiota require various culture techniques that are time-consuming and laborious. Nasmyth et al[7] compared fecal bacterial compositions among 11 pouches and 12 ileostomies using conventional culture techniques. They found a significant increase in numbers of anaerobic bacteria such as *Bacteroides* and *Bifidobacteria* in pouch-derived samples. Individual strains of fecal anaerobic bacteria in 7 ileostomies, 9 ileal pouches with UC, and 5 ileal pouches with FAP were also investigated by Smith et al[8] using conventional culture methods. They demonstrated that the ratio of strict to facultative anaerobes within the UC pouch was maintained relative to UC stoma. Even with modern culture techniques, however, most commensal bacteria are difficult to culture because of the strict anaerobic and complex environment required for the growth of many species. For this reason, culturable bacteria are limited to between 20% and 30% of the total residential bacteria.[9,10] It is possible that nonculturable microbiota, rather than culturable ones, play major roles in the physiologic and pathologic events that occur in the pouch after TPC.

Terminal restriction fragment length polymorphism (T-RFLP) analysis is an alternative molecular approach that allows assessment of the diversity of a bacterial community and of different ecosystems.[11-13] T-RFLP analysis allows rapid recognition of complex bacterial communities, which are depicted in the patterns and profiles of terminal restriction fragments (T-RFs). Although T-RFLP analysis does not necessarily identify specific bacterial species directly, both culturable and nonculturable species of microorganisms are distributed into clusters based on the migration pattern and relative sizes of enzyme-restricted genomic DNA fragments on gel electrophoresis. T-RFLP analysis is advantageous for assessing the diversity of fecal microbiota because many samples can be treated at one time and community structure among individual microorganisms can be easily compared.[11,12,14]

The aims of this study were 2-fold: (1) use T-RFLP analysis to investigate the diversity of bacterial communities in fecal samples from patients with an ileostomy, those with a relatively newly formed ileal pouch (within 2 years of stoma closure), those with an established ileal pouch (more than 2 years since stoma closure), and control healthy volunteers; (2) evaluate changes in bacterial composition in the ileal pouch over time.

MATERIALS AND METHODS

Samples. Samples were collected from 49 patients who had undergone TPC with IPAA (all for UC) and 31 healthy volunteers (Table I). Diagnosis of UC was based on a combination of clinical symptoms, endoscopic findings, and histologic examination. None of the healthy volunteers was treated with any medications. At Tohoku University Hospital, patients with UC underwent routinely a 2- or 3-step operative approach, after which the ileal pouch becomes "functional" after complete closure of the covering loop ileostomy. An ileal pouch was termed a "functional pouch" when stool was excreted from the anus just after closure of the loop ileostomy.

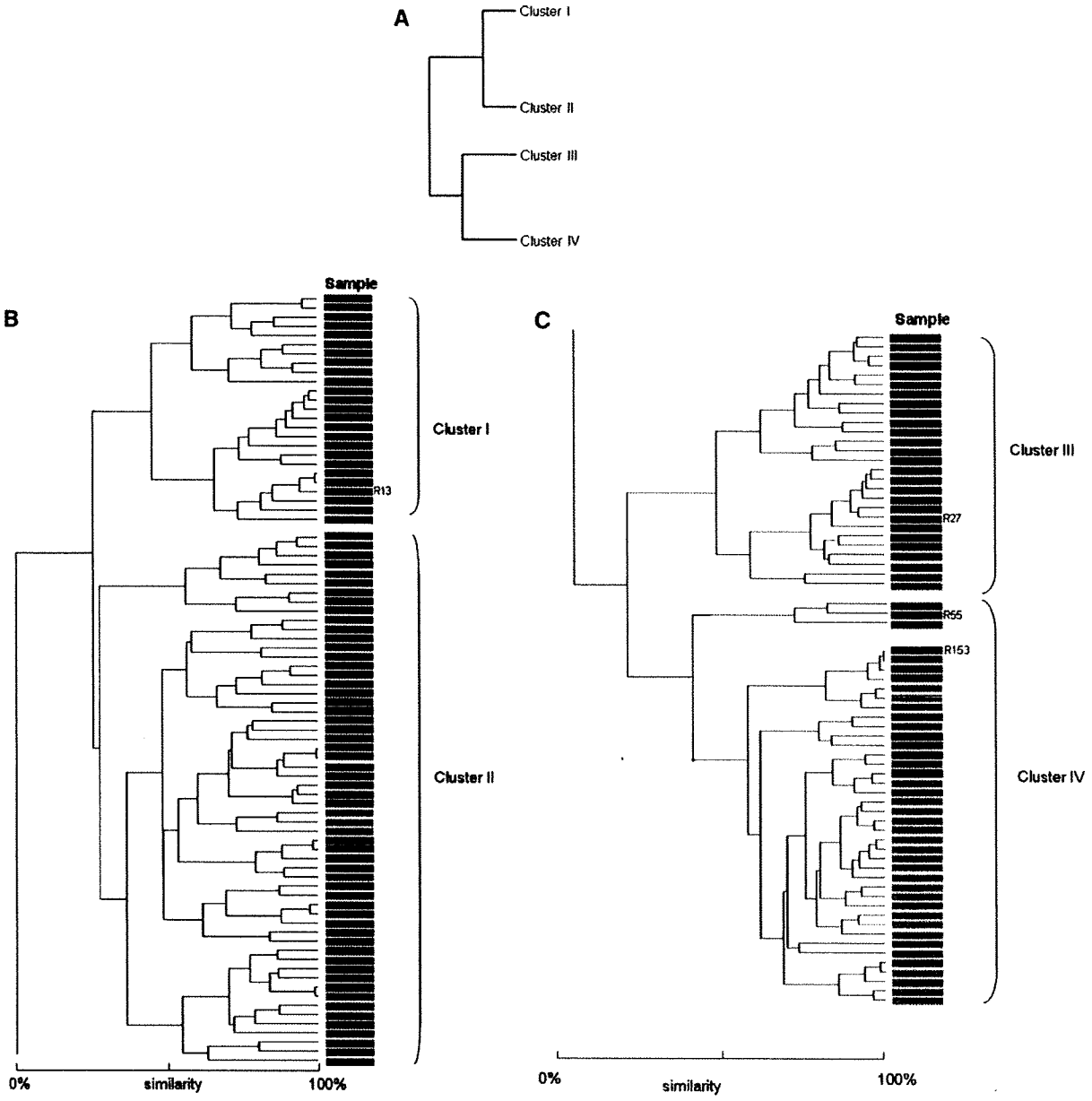

Fig 1. Dendrogram of fecal bacteria species using samples from ileostomy, ileal pouch less or more than 2 years after ileostomy closure, and controls. Terminal restriction fragment length polymorphism (T-RFLP) patterns following *Hha*I or *Msp*I digestion were analyzed using the Pearson correlation coefficient and the unweighted pair group method with arithmetic mean algorithm. (*A*) Samples were divided into 2 major clusters. Each cluster was further divided into 2 subclusters. (*B*) and (*C*) Samples from the ileostomy, the ileal pouch within 2 years of ileostomy closure, the ileal pouch 2 or more years after ileostomy closure, or the control group are indicated by a black, blue, red, or green box, respectively. R13, R27, R55, and R153 indicate samples that were obtained from the same patient "R" at 13, 27, 55, and 153 days after ileostomy closure, respectively.

Samples were divided into 1 of 4 groups: 34 samples from patients with end ileostomy or loop ileostomy (11 and 2 patients, respectively), 73 from 25 patients with an ileal pouch within 2 years after stoma closure, 13 samples from 11 patients with an ileal pouch more than 2 years after stoma closure, and 31 rectal stools from 31 healthy volunteer controls. We obtained multiple samples from the same patient under different conditions such as with ileostomy or with an ileal pouch before or more than 2 years after ileostomy closure. The number of bowel movements averaged from 6 to 8

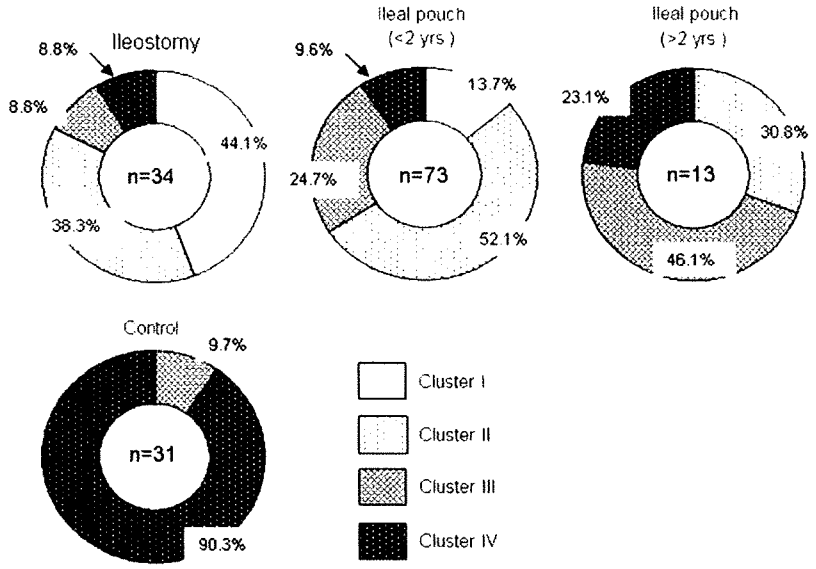

Fig 2. Frequency of samples from the ileostomy, the ileal pouch within 2 years after stoma closure, the ileal pouch more than 2 years after stoma closure, and the control groups that fall within Clusters I–IV. Note that 44% of the ileostomy samples fell into Cluster I and that 90% of the control samples grouped in Cluster IV. Microbes from more than 80% of ileostomy stool samples grouped into Clusters I or II.

(range, 5–10) in patients with an ileal pouch within 2 years and less than 6 in all patients with a pouch more than 2 years after ileostomy closure. Of 13 ileostomy patients, 12 received prednisolone (10–40 mg/day) at the time of sampling, as well as antibiotics (cefotiam hydrochloride, 2 g/day) until the fourth postoperative day. Output volume from the ileostomy was approximately 500 to 1,500 ml per day in the first week and 1,200 to 2,000 ml after 2 weeks following ileostomy construction.

Patients with an ileal pouch (less or more than 2 years after stoma closure) who were tested in the study were free from surgical complications and clinical symptoms that might indicate pouchitis, such as increase of bowel movements more than usual and contamination of blood in stool; alternatively, evidence of pouchitis was neglected during endoscopic examination. Fecal samples were obtained under informed consent, and the study was approved by the ethics committee of Tohoku University, Graduate School of Medicine.

DNA extraction from fecal samples. Fecal samples were kept at –80°C until DNA extraction. Fecal samples (20 mg) were washed 3 or 4 times in 500 μL of Tris ethylenediaminetetraacetic acid (TE) buffer (pH 8.0) and centrifuged at 14,000*g* for 5 minutes at each washing step. After the final wash, fecal pellets were resuspended in 600 μL TE. A total of 100 μL of 10% sodium dodecyl sulfate, 300 mg of glass beads (diameter, 0.1 mm), and 600 μL of buffer-saturated phenol were added to the suspension, and the mixture was vortexed vigorously for 10 seconds and then incubated at 70°C for 10 minutes. This extraction was repeated 2 more times.

After a final centrifugation at 14,000*g* for 5 minutes, 400–600 μL of the aqueous supernatants were transferred to a fresh tube. DNA was precipitated with 600 μL isopropanol and 40–60 μL of 3 M sodium acetate at room temperature for 5 minutes and pelleted at 14,000*g* for 5 minutes. The resulting pellets were washed with 70% ice-cold ethanol twice, dried, and finally resuspended in 200 μL of TE buffer. DNA was purified further using the High Pure Polymerase Chain Reaction (PCR) Template Preparation kit (Roche, Basel, Switzerland) according to the manufacturer's protocol and then eluted in 50 μL of the PCR template elution buffer supplied with the kit (Roche).

PCR amplification and T-RFLP analysis. A forward primer, 27F (5′-AGAGTTTGATCCTGGCT CAG-3′) and a reverse primer, 1492R (5′-GGTTAC CTTGTTACGACTT-3′) were used to amplify the consensus sequence of bacterial 16S rRNA genes. The forward primer labeled at the 5′ end with 6-carboxyfluorescein was synthesized by Applied Biosystems, Tokyo, Japan. To carry out PCR, 10 ng of DNA from each stool sample was placed

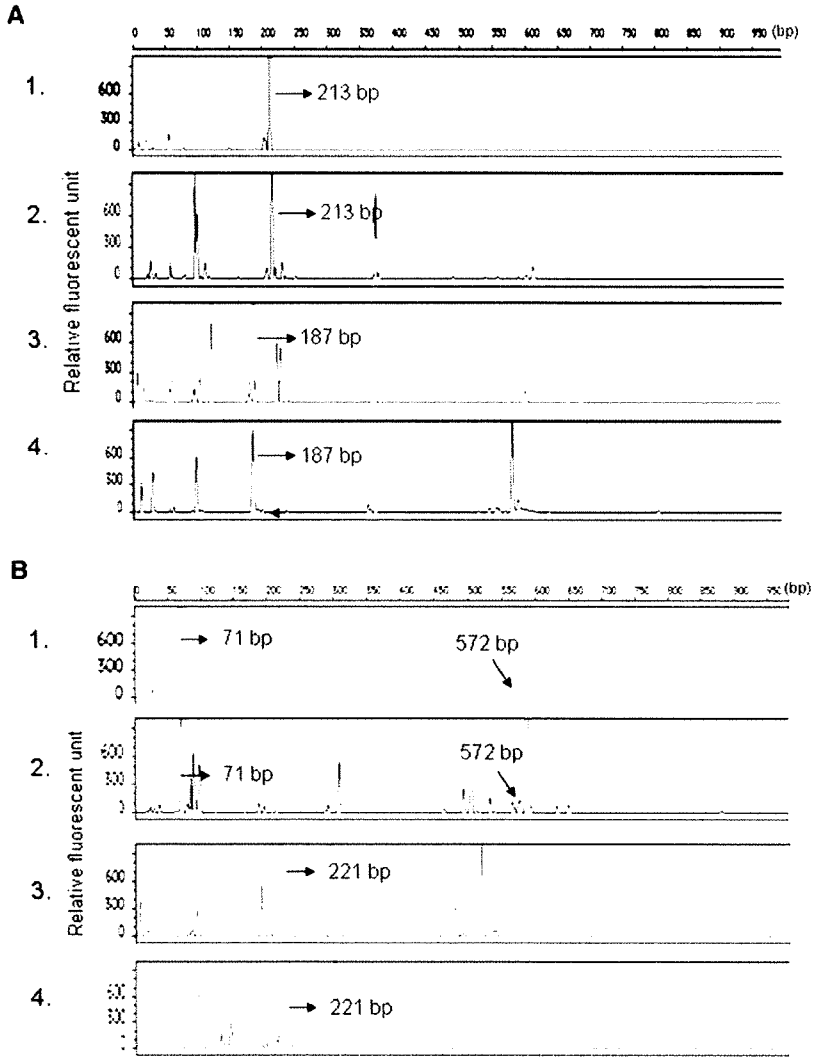

Fig 3. Terminal restriction fragment length polymorphism (T-RFLP) analysis patterns of DNA from ileostomy, ileal pouch, and control samples after digestion with *Hha*I (*A*) or *Msp*I (*B*). The horizontal axis indicates the relative length of DNA fragments (bp). The vertical axis indicates the relative fluorescence emitted by the band. Lane 1 shows results from an ileostomy sample; lanes 2 and 3 show results from ileal pouch samples from the patient "R" at 13 days (*lane 2*) or 153 days (*lane 3*) after ileostomy closure. Lane 4 is derived from a control sample. *A*, Note that the 213-bp *Hha*I T-RF (*arrows*) was detected in lanes 1 and 2, but not in lanes 3 and 4. In contrast, the 187-bp *Hha*I T-RF (*arrows*) was present in samples on lanes 3 and 4, but absent from lanes 1 and 2. *B*, Note that the 71-bp and 572-bp *Msp*I T-RFs (*arrows*) were detected in lanes 1 and 2, but absent in lanes 3 and 4. In contrast, a 221-bp *Msp*I T-RF (*arrows*) was present in lanes 3 and 4, but absent in lanes 1 and 2.

in a T-gradient thermal cycler (Biometra, Goettingen, Germany), and the target DNA was amplified according to the protocol described by Sakamoto et al.[12] In brief, DNA was denatured initially at 95°C for 3 minutes and then passed though 30 cycles of 95°C for 30 seconds, 50°C for 30 seconds, and 72°C for 90 seconds, with a final extension period at 72°C for 10 minutes. The 16S rRNA gene amplification products were purified by polyethylene glycol 6000 (PEG 6000) precipitation, and the resulting pellets were resolved in 20 μL of distilled water.

Restriction enzymes were selected from a report by Moyer et al.[15] Purified PCR products (2 μL) were digested with 20 U of either *Hha*I or *Msp*I (Takara Shuzo, Kyoto, Japan) at 37°C for 3 hours. The length of T-RFs was determined using an ABI PRISM 3100 genetic analyzer (Applied Biosystems) in GeneScan mode. Standard size markers (such as GS 500 ROX and GS 1000 ROX; Applied

Table II. Duration from ileostomy closure to stool sampling

Cluster	*Duration (d)*	*Range (d)*
I	11.0*	8–24
II	55.5**	11–150
III	264.5	115–661
IV	310.0	55–2159

*Significantly ($P < .01$) shorter than the others.
**Significantly ($P < .01$) shorter than Cluster III and IV.

Table III. Number of T-RFs

Group	*Hha I digestion*	*Msp I digestion*
Ileostomy ($n = 34$)	14.5 (10–21)	18.5 (10–22)
Ileal pouch (<2 y after IC) ($n = 73$)		
0–31 d ($n = 26$)	13.0 (8–18)	13.5 (8–20)
31–100 d ($n = 21$)	22.0 (16–29)	20.0 (13–23)
101 d–2 y ($n = 26$)	16.0 (12–21)	17.0 (12–24)
Ileal pouch (>2 y after IC) ($n = 13$)		
Control ($n = 31$)	36.0* (27–45)	41.0* (28–48)

IC, Ileostomy closure.
*More than the others ($P < .01$).

Biosystems) were used, and fragment sizes were estimated using the local Southern method in GeneScan 3.1 software (Applied Biosystems). The major T-RFs were identified by computer analysis using a combination of 3 tools: (1) a T-RFLP analysis program developed by Marsh et al[16] and published on the web, (2) a phylogenetic assignment database for T-RFLP analysis of human colonic microbiota (PAD-HCM),[17] and (3) Microbiota Profiler (InfoCom T-RFLP Database & Analysis Software; InfoCom Co., Tokyo, Japan). Peaks with a height of < 25 FU were excluded from the analysis. *Hha*I or *Msp*I T-RFLP patterns were displayed for the cluster analyses using the Microbiota Profiler (InfoCom). Cluster distances were calculated using the Pearson correlation coefficient and the unweighted pair group method with arithmetic mean (UPGMA). These statistical methods were used to generate a dendrogram graphic that demonstrates similarities between samples.

Qualitative and semiquantitative analysis of fecal bacteria in T-RFLP. For T-RFLP analyses, the number of peaks from each display was counted, and medians within each group were calculated. Furthermore, the detection frequency of specific T-RFs was calculated. The amount of bacterial DNA represented by each peak was measured semiquantitatively from the area per individual T-RF peak relative to the total T-RF peak areas, which was expressed as the percentage of the area under the peak curve (%AUC).[18,19]

Specific PCR for detection of *C. coccoides* group. We used gene-specific PCR amplification to confirm the presence of *C. coccoides* groups predicted by PAD-HCM and represented by the 187-bp T-RFs in *Hha*I digestions. A total of 3 independent experiments were performed using 3 samples each (12 total) from patients with ileostomy, ileal pouch within 30 days after ileostomy closure, ileal pouch more than 100 days after ileostomy closure, and controls (healthy volunteers), respectively. The sequence of *C. coccoides* group–specific primers were reported previously (forward: 5′-AAATGACGGTACCTGAC TAA-3′ and reverse: 5′-CTTTGAGTTTCATTCTTG CGAA-3′).[20] A total of 2 μL DNA from stool was used as a template in a 25-μL PCR mixture containing 1.25 U of TaKaRa Ex Taq DNA polymerase (Takara Shuzo) according to the manufacturer's protocol. The amplification program included 1 cycle of 94°C for 5 minutes, 25 cycles of 94°C for 20 seconds, 50°C for 20 seconds, and 72°C for 50 seconds, and 1 final cycle of 72°C for 5 minutes. DNA samples extracted from *Ruminococcus productus* (JCM 1471; Japan Collection of Microorganisms, Saitama, Japan) or *Bifidobacterium adolescentis* (JCM 7045) were used as positive or negative controls, respectively. After electrophoresis on 1% agarose gels, amplification products were stained with ethidium bromide for imaging.

Statistical analysis. Values were presented as median and percentile or mean ± SE. The Mann-Whitney *U* test was used to determine if there was a significant correlation between the duration of functional pouch after ileostomy closure and the number of T-RFs. The frequencies of selected peaks in T-RFLP were compared using the Fisher exact test. Significance was accepted at $P < .05$.

RESULTS

Recovery of the fecal DNA. Adequate quantities and quality of DNA samples were obtained from watery stool samples. DNA concentrations ranged between 10.5 (±2.1) ng/mg stool in the ileostomy group, 14.8 (±2.3) ng/mg in patients with a new ileal pouch (within 2 years of ileostomy closure), and 30.1 (±7.7) ng/mg in patients with an established ileal pouch (>2 years since ileostomy closure). In contrast, DNA concentrations in the control group averaged 920.9 (±320.9) ng/mg.

T-RFLP analysis and clustering of fecal bacteria. Diversity of bacterial composition in fecal samples were compared in a dendrogram generated in Microbiota Profiler (InfoCom) using the Pearson

Table IV. Bacterial candidates corresponding to the "colonic" peak, *Hha*I-treated 187-bp, and *Msp* I-treated 221-bp T-RFs

Bacterial species	*Strain/clone*	*%sim*	*Accession no.*	*Group*
Ruminococcus obeum		98.24	AB084766	ClostridiumXIVa
Uncultured bacterium	HuCA5	98.62	AJ408961	ClostridiumXIVa
Uncultured human intestinal bacterium	JW2E8	99.61	AB080870	ClostridiumXIVa
Uncultured bacterium	38E09		AB181447	ClostridiumXIVa
Uncultured Ruminococcus sp.	NO44	99.22	AB064754	ClostridiumXIVa
Uncultured Ruminococcus sp.	NB288	98.83	AB064761	ClostridiumXIVa
Ruminococcus gnavus		98.21	L76597	ClostridiumXIVa
Uncultured firmicute	NB4F10	98.04	AB064778	ClostridiumXIVa
Uncultured Ruminococcus	NB4C1	99.61	AB064765	ClostridiumXIVa
Uncultured bacterium	p-2746-24E5	99.4	AF371546	ClostridiumXIVa
Ruminococcus obeum	1-33	98.05	AY169419	ClostridiumXIVa
Uncultured Ruminococcus sp.	NO3	98.64	AB064755	ClostridiumXIVa
Ruminococcus sp.	CO12	98.83	AB064896	ClostridiumXIVa
Eubacterium halii		99.41	L34621	ClostridiumXIVa
Uncultured bacterium	OLDA-B9	99.8	AB099741	ClostridiumXIVa
Ruminococcus (peptostrept) products			D14144	ClostridiumXIVa
Clostridium Xylanolyticum			X76739	ClostridiumXIVa
Clostridium algidixylanolyticum			AF092549	ClostridiumXIVa
Clostridium saccharolyticum			Y18185	ClostridiumXIVa
Clostridium saccharolyticum			M59112	ClostridiumXIVa
Uncultured Ruminococcus sp.	NB2B8		AB064761	ClostridiumXIVa
Uncultured Ruminococcus sp.	NB2E8		AB064760	ClostridiumXIVa
Uncultured human intestinal bacterium	JW1B11		AB080869	ClostridiumXIVa
Uncultured human intestinal bacterium	JW1D8		AB080871	ClostridiumXIVa
Uncultured firmicute	NO78		AB064771	ClostridiumXIVa
Uncultured firmicute	NS2G4		AB064712	ClostridiumXIVa
Uncultured human intestinal bacterium	JW1H4		AB080873	ClostridiumXIVa
Uncultured bacterium	OLDA-E8		AB099736	ClostridiumXIVa
Uncultured firmicute	NO1D2		AB064774	ClostridiumXIVa
Uncultured firmicute	NO33		AB064777	ClostridiumXIVa
Human intestinal firmicute	CO4		AB064888	ClostridiumXIVa
Roseburia intestinalis	str.L1-82T		AJ312385	ClostridiumXIVa
Uncultured firmicute	NO1B9		AB064718	ClostridiumXIVa

T-RF, Terminal restriction fragment; *%sim*, similarity to the reported DNA sequence.

correlation coefficient and the UPGMA algorithm (Fig 1). Samples were divided into 2 major clusters, each cluster was further divided into 2 subclusters, and the 4 groups (containing 25, 58, 27, or 41 samples, respectively) were designated as Clusters I, II, III, and IV (Fig 1, *A–C*). Because intestinal epithelial changes after TPC are characterized by a time-dependent transformation to a more colonic phenotype, we investigated whether the diversity of microbes in each subcluster showed a deviation toward a colonic or small intestinal bacterial community. Most of the ileostomy samples were categorized into Cluster I or II (Fig 2), and less than 10% of ileostomy samples were classified into Cluster IV. In contrast, more than 90% of the control samples were grouped in Cluster IV. These results suggest that Clusters I and IV feature ileal and colonic populations of microbiota, respectively. Similarly, as the time since ileostomy closure increased, the ratio of samples in Cluster III also increased—from 25% for ileal pouch with ileostomy closure within 2 years to 46% for samples from ileal pouch more than 2 years (Fig 2).

Within each cluster, we calculated the duration from ileostomy closure to stool sampling from pouches (Table II). The median duration in Clusters I, II, III, and IV were significantly different at 11, 56, 265, and 310 days, respectively. Interestingly, in analyses of multiple samples from the same patients at different time points, the interval of time after ileostomy closure appeared to affect sample clustering more potently than individual characteristics of bacterial communities. A typical example can be observed in samples from the

Table V. Detection rate of representative T-RFs in Hha I digestion

		Ileostomy (n = *34*)		*Ileal pouch (<2 years)* (n = *73*)			
				0–30 days (n = *26*)		*31–100 days* (n = *21*)	
T-RF size (op)	*Bacteria predicted by PAD-HCM*	*+%*	*%AUC*	*+%*	*%AUC*	*+%*	*%AUC*
Colonic fragments							
31	Unclassified bacteria	11.8	2.0 ± 1.4	3.8	0.5	14.3	2.8 ± 1.2
61	Mesorhizobium, Lactobacilli, peptosterptococcus, etc.	23.5	4.8 ± 2.8	11.5	3.6 ± 2.4	23.8	7.3 ± 4.6
97	Bacteriodes, verrucomicrobia, etc.	55.9	8.1 ± 2.4	53.8	5.6 ± 1.7	52.4	4.2 ± 1.3
187	Ruminococcus, Clostridium, Eubacterium, uncultured bacterium, etc.	32.4	16.1 ± 7.2	3.8	39.6*	52.4	10.1 ± 2.6
224	Clostridium, uncultured Clostridium, etc. Lactobacilli	29.4	1.7 ± 0.5	34.6	6.2 ± 3.5	28.6	2.0 ± 1.0
367	Bifidobacterium, etc.	50.0	21.9 ± 5.4	73.1	33.1 ± 6.4	85.7	29.1 ± 5.4
376	Eubacterium uncultured bacterium, etc.	0.0		0.0		4.8	0.7
567	Uncultured Eubacterium, Lactobacilli, etc.	0.0		0.0	0.5	4.8	1.1
588	Vellonella, uncultured bacteria	11.8	8.9 ± 3.4	19.2	9.0 ± 2.0	14.3	58.4 ± 28.9
Ileal fragments							
213	Unknown bacteria	85.3	41.0 ± 0.1	92.3	27.5 ± 4.9	66.7	5.7 ± 1.3
Common fragments							
57	Unclassified bacteria	88.2	3.8 ± 0.5	69.2	2.6 ± 0.4	71.4	3.3 ± 10.8

VE+ %, ve positive rate(%); *AUC*, area under the peak curve; *T-TRF*, terminal restriction fragment.
T-RFs ranging from 27 to 926 bp were selected according to their positive rate(>70%) in "colonic," "ileal," or "common" peak, respectively.
*Note that %AUC was calculated from 1 sample.

patient "R," wherein the cluster pattern of each sample correlated closely with the duration of the "functional pouch" (Fig 1, *B* and *C*).

Characteristics such as age and sex were not applied in the cluster derivations. Samples from the patients who had received prednisolone, antibiotics (cefotiam hydrochloride), or probiotics fell into Cluster I at a significantly greater percentage than those patients without drugs (data not shown).

T-RFLP patterns digested with *Hha*I or *Msp*I in samples from the ileostomy, the ileal pouch, and the control groups. Typical T-RFLP patterns created by both *Hha*I and *Msp*I digestion are shown in Fig 3. In this Figure, the samples were obtained from the ileal pouch of the same patient (patient "R") at different times after ileostomy closure.

The number of T-RFs in *Hha*I- or *Msp*I-digested samples from patients with ileostomy, ileal pouch within or more than 2 years after stoma closure, or control volunteers were compared. With either enzyme treatment, the control group exhibited almost twice the number of T-RFs than any other group (Table III). In contrast, there was no significant difference in the number of T-RFs among patients with ileostomy, ileal pouch within 2 years after ileostomy closure, and ileal pouch more than 2 years after ileostomy closure.

The specific T-RFs, a 213-bp *Hha*I T-RF, a 71-bp *Msp*I T-RF, and a 572-bp *Msp*I T-RF were detected preferentially in ileostomy and in the ileal pouch samples taken earlier after ileostomy closure. In contrast, a 187-bp *Hha*I and a 221-bp *Msp*I T-RF

Table V. *continued*

Ileal pouch (<2 years) (n = *73*)		*Ileal pouch*			
101 days–2 years (n = *26*)		*(>2 years)* (n = *13*)		*Control* (n = *31*)	
+%	*%AUC*	+%	*%AUC*	+%	*%AUC*
0.0		7.7	0.8	90.3	8.4 ± 1.4
50.0	5.5 ± 1.0	15.4	3.0 ± 0.8	87.1	1.5 ± 0.6
42.3	3.8 ± 0.8	30.8	14.5 ± 11.6	83.9	3.9 ± 1.4
84.6	24.0 ± 4.2	92.3	26.7 ± 3.6	100.0	32.6 ± 3.2
80.8	4.5 ± 0.9	53.8	4.3 ± 1.5	90.3	3.5 ± 0.6
84.6	31.8 ± 4.3	84.6	25.4 ± 4.9	83.9	9.0 ± 2.8
11.5	2.1 ± 0.9	7.7	0.9	83.9	1.2 ± 0.2
7.7	1.5 ± 0.6	0.0		90.3	9.5 ± 0.8
26.9	16.4 ± 9.3	23.1	4.8 ± 1.6	90.3	8.1 ± 1.8
42.3	15.6 ± 7.5	30.8	3.2 ± 0.9	12.9	0.2 ± 0.1
80.8	2.7 ± 0.5	61.5	5.7 ± 2.0	90.3	2.0 ± 0.3

were observed predominantly in samples from patients with a later-stage ileal pouch or from controls (Fig 3, *A* and *B*). These examples demonstrate that the presence or absence of particular T-RFs in the ileal pouch can depend on the time of sampling after ileostomy closure.

Access to PAD-HCM[17] showed that the presence of both a 187-bp *Hha*I T-RF and a 221-bp *Msp*I T-RF is a hallmark of *Clostridium* rRNA subcluster XIVa. The 213-bp *Hha*I T-RF and the 71-bp and 572-bp *Msp*I T-RFs did not correspond to the bacterial species listed in this database (Table IV).

Definition of "colonic," "ileal," and "common" fragments and detection rates of those fragments. As shown in Fig 3, specific differences in T-RFLP patterns were detected between samples from ileostomy patients and controls. Based on their appearance in different sample groups, T-RFs were divided into 3 groups classified previously in a study of epithelial gene expression.[2] We defined positive rate percentage as detection frequencies and %AUC referred to rate (%) of area under the peak curve in total area in Tables V and VI. Fragments found predominantly in control samples (ie, "colonic" fragments) were defined by T-RFs detected in more than 70% of control samples and with a detection frequency greater ($P < .05$) than that of the ileostomy. Fragments found predominantly in the ileostomy (ie, "ileal" fragments) were defined as T-RFs detected in more than 70% of ileostomy samples and with a detection frequency greater ($P < .05$) than that of controls. "Common" fragments were defined as T-RFs that were found in more than 70% of both ileostomy and control samples, with no significant difference in detection frequencies.

Table VI. Detection rate of representative T-RFs in Msp I digestion

				Ileal pouch (<2 years) (n=73)						*Ileal pouch (<2 years)*		*Control*	
		Ileostomy (n = 34)		*0–30 days (n = 26)*		*31–100 days (n = 21)*		*101 days–2 years (n = 26)*		n = 13		n = 31	
T-RF size (bop)	*Bacteria predicted by PAD-HCM*	+%	*%AUC*	+%	*%AUC*	+%	*%AUC*	+%	*%AUC*	+%	*%AUC*	+%	*%AUC*
Colonic fragments													
144	Uncultured Eubacterium, etc.	8.8	1.4 ± 0.7	11.5	1.6 ± 0.8	33.3	1.1 ± 0.3	11.5	1.0 ± 0.2	30.8	2.0 ± 1.1	77.4	2.3 ± 0.4
221	Ruminococcus, Clostridium, Eubacterium, uncultured bacterium, etc.	32.4	18.1 ± 7.8	3.8	36.*9	57.1	13.1 ± 2.8	88.5	25.3 ± 4.1	92.3	25.6 ± 4.8	100.0	41.1 ± 3.1
287	Clostridium, Uncultured bacterium, etc.	5.9	1.2 ± 0.7	30.8	3.1 ± 1.1		0.0	30.8	0.8 ± 0.2	30.8	2.0 ± 0.9	90.3	11.2 ± 1.7
297	Ruminococcus, Clostridium, Uncultured bacterium, etc.	26.5	1.5 ± 0.6	7.7	14.9 ± 9.7	19.0	1.6 ± .08	73.1	5.5 ± 1.4	76.9	1.8 ± 0.5	100.0	25 ± 0.5
299	Ruminococcus, Megasphaera, vellonella, Uncultured bacterium, etc.	44.1	2.3 ± 0.7	26.9	1.8 ± 1.0	28.6	2.5 ± 0.8	38.5	1.6 ± 0.5	23.1	1.6 ± 0.7	87.1	3.8 ± 0.7
309	Uncultured bacterium	11.8	0.9 ± 0.3	3.8	1.0	14.3	1.5 ± 0.9	30.8	2.3 ± 0.6	53.8	1.9 ± 0.3	100.0	4.2 ± 0.5
481	Unclassified bacteria	2.9	1.7	23.1	1.8 ± 0.6	9.5	4.2 ± 1.4	19.2	2.9 ± 1.4	15.4	5.9 ± 2.1	93.5	3.0 ± 0.3
Ileal fragments													
71	Uncultured bacterium	82.4	16.1 ± 3.9	50.0	9.5 ± 3.0	14.3	1.6 ± 0.1	30.7	5.3 ± 3.0	15.4	0.8 ± 0.5	25.8	0.4 ± 0.1
572	Lactobaccilli, etc.	91.2	24.8 ± 4.8	76.9	19.5 ± 4.4	76.2	4.5 ± 1.2	34.6	3.9 ± 2.0	23.1	2.9 ± 0.6	29.0	1.0 ± 0.2
Common fragments													
559	Streptococcus, etc.	73.5	21.7 ± 4.2	69.2	20.7 ± 5.5	76.2	40.4 ± 7.9	65.3	18.5 ± 4.6	76.9	25.9 ± 7.0	83.9	7.8 ± 1.8

VE+ %, ve positive rate(%); *AUC*, area under the peak curve; *T-RF*, terminal restriction fragment.
T-RFs ranging from 27 to 926 bp were selected according to their positive rate(>70%) in "colonic," "ileal," or "common" peak, respectively.
*Note that %AUC was calculated from 1 sample.

According to these criteria, use of *Hha*I as a digestion enzyme resulted in 9 T-RFs (31, 61, 97, 187, 224, 367, 376, 567, and 588 bp) classified as "colonic" fragments, 1 fragment (213-bp T-RF) as an "ileal" fragment, and 1 fragment (57-bp T-RF) as a "common" fragment (Table V). Searches of PAD-HCM demonstrated that the "colonic" fragments could include DNA from *Lactobacillus, Ruminococcus, Clostridium, Eubacterium, Bacteroides, Bifidobacterium,* and others. Sizes of the "ileal" fragment and the "common" fragment did not match any bacterial DNA T-RFs listed in PAD-HCM. *Msp*I digestion resulted in 7 T-RFs (144, 221, 287, 297, 299, 309, and 481 bp) classified as "colonic," 2 fragments (71- and 572-bp T-RFs) as "ileal," and 1 fragment (559-bp T-RF) as "common" (Table VI). The "colonic" fragments corresponded to bacterial species similar to those seen in the *Hha*I treatment. The "ileal" fragments were predicted to belong to *Lactobacillus* or a nonculturable bacterium. The "common" fragments were matched to *Streptococcus* as well as unmatched bacteria in this database.

One 187-bp *Hha*I and 3 *Msp*I "colonic" fragments (221, 297, and 309 bp) were detected in all control samples. When we evaluated the relative frequency of detection of those peaks in samples from the ileal pouch, these particular "colonic" fragments were detected more often as the time after ileostomy closure increased (Tables V and VI); however, the detection rate of the other "colonic" fragments did not exhibit remarkable changes. In contrast, detection of 213-bp *Hha*I and 572-bp *Msp*I "ileal" fragments decreased with time after

ileostomy closure (Tables V and VI). The frequency of detection for "common" fragments was essentially stable at all stages after ileal pouch formation.

In samples from the established ileal pouch, the %AUC of the 187-bp *Hha*I and the 221-bp *Msp*I "colonic" fragments exceeded 25%, indicating that a substantial percentage of bacteria in the ileal pouch showed "colonic" preference. In contrast, although some other "colonic" fragments showed increased incidence (Tables V and VI), the %AUC of these other fragments did not increase. For "ileal" fragments in the ileal pouch, %AUC generally paralleled detection rates of the peaks, suggesting that populations of ileal pouch bacteria characterized by "ileal" markers decreased with time.

Specific PCR for the detection of *C. coccoides* group. 187-bp *Hha*I and 221-bp *Msp*I "colonic" fragments were predicted to correspond to DNA sequence from *Clostridium* rRNA subcluster XIVa, which corresponds to a gene in the *C. coccoides* group.[21] Of the 33 species predicted, 21 (64%) were not culturable bacteria (Table IV), and PCR was used to score for the presence or absence of the rRNA gene. A 440-bp *C. coccoides* amplification product (as predicted) was observed in all samples from an ileal pouch more than 100 days after ileostomy closure and from a control (Fig 4), but no product was detected from ileostomy samples or those from the ileal pouch within 30 days of ileostomy closure.

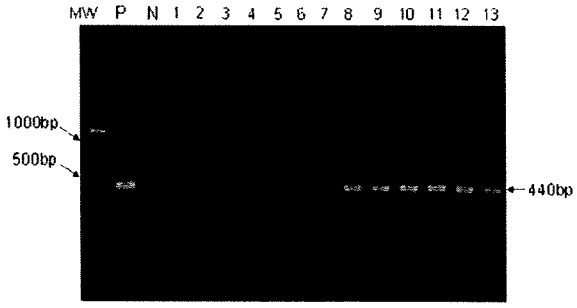

Fig 4. Detection of a 16S ribosomal RNA gene amplification product specific to the *C. coccoides* group. A 16S ribosomal RNA gene specific to the *C. coccoides* group was amplified using the gene-specific primers. Amplified products were analyzed by 1% agarose gel electrophoresis and stained with ethidium bromide. *Lane MW*, 100-bp DNA marker (Takara Shuzo); *lane P*, positive control (DNA samples from *Ruminococcus productus;* Japan Collection of Microorganisms [JCM 1471]); *lane N*, negative control (DNA samples from *Bifidobacterium adolescentis*; JCM 7045); *lanes 1–3*, DNA samples from the ileostomy; *lanes 4–6*, DNA samples from the ileal pouch 7, 10, or 13 days after ileostomy closure, respectively; *lanes 7–9*, DNA samples from the ileal pouch 153, 255, or 262 days after ileostomy closure, respectively; *lanes 10–12*, DNA from feces of healthy volunteers; *lane 13*, distilled water.

DISCUSSION

First of all, this study was intended to display the difference of fecal bacterial communities between samples from the ileostomy, ileal pouch, and colon. In a dendrogram analysis, stool samples from patients with ileostomy, with an ileal pouch within or more than 2 years after ileostomy closure, and from controls were categorized into 4 clusters. In further analyses of clustering of samples from the ileal pouch, we found that the median time of formation of a "functional" pouch after ileostomy closure was significantly different between the 4 clusters. This observation suggests that the "age" of a functioning pouch is likely to be a determining factor in cluster affiliation of pouch microbes.

Among ileal pouch samples, Clusters I, II, III, and IV all demonstrated changes in microbial diversity with increasing time since ileostomy closure. Ongoing treatments of patients in the ileostomy group with prednisolone, antibiotics (cefotiam hydrochloride), or probiotics might be factors that contribute to differences between Cluster I and other clusters. Other uncontrolled clinical factors, such as presence of severe mucosal inflammation in the resected colon or perioperative fast, might also affect clustering. Because patients with relatively new pouches who did not receive drugs were classified into Cluster I, it is unlikely that these factors influence clustering strongly. In contrast, consistent collection of samples from ileal flow without stasis and proper timing of sampling after the initiation of pouch function appear to be essential for accurate classification.

Focusing on the presence or absence of specific T-RFs, a 213-bp *Hha*I T-RF, a 71-bp *Msp*I, and a 572-bp *Msp*I T-RF were detected preferentially in ileostomy, and the ileal pouch samples taken early after ileostomy closure. In contrast, a 187-bp *Hha*I T-RF and a 221-bp *Msp*I T-RF were observed predominantly in samples from patients with a late-stage ileal pouch or from controls. These data indicate that shifting in bacterial composition in the ileal pouch from "ileal" to "colonic" is time-dependent and is mediated both by decreases in predominantly ileal bacteria and increases in predominantly colonic bacterial species. Because not all "colonic" fragments increased in number or %AUC with

increasing duration after ileostomy closure, we suggest that only selected bacteria with colonic preferences can grow in the ileal pouch. In contrast, decreases in the number or %AUC of "ileal" fragments were relatively common among bacteria with an "ileal" preference.

Members of the *C. coccoides* group, including nonculturable bacteria, were not detected in samples from the ileostomy, but clear evidence of DNA from this group was found in the ileal pouch more than 100 days after ileostomy closure. In previous reports using bacterial culture techniques,[7,8] the numbers of culturable *Clostridium* spp. and *Clostridium perfringens* in the ileal pouch 3 months after ileostomy closure were similar to those in the ileostomy. The results of our study indicate that changes in the composition of fecal bacterial communities in the ileal pouch are complex and that there are limitations to conventional culture methods; a DNA-based approach offers a powerful advantage in studying fecal bacterial communities.

The distribution of these gut bacteria also changes with some inflammatory conditions. For example, cell numbers of the *C. coccoides* group were significantly greater in fecal samples from celiac infants than from age-matched healthy subjects.[22] Cell numbers of the *C. coccoides* group have been reported to increase in tissue sections from patients with UC and Crohn disease relative to controls without inflammatory bowel disease.[23] Because pouchitis is thought to be the most frequent complication with a pelvic pouch, changes in microbial components in the ileal pouch such as an increase of the *C. coccoides* group may be associated with triggering and/or amplifying pouch inflammation. Understanding the composition of bacteria in a healthy pouch without inflammation is an essential part of investigating the pathogenesis of pouchitis.

Functional roles for altered microbiota communities in epithelial cell-bacteria interactions have not been determined. It has been suggested, however, that growth of *Clostridium* spp. can lead to enhancement of short chain fatty acid concentrations in the ileal pouch,[24,25] which may result in modulation of epithelial gene expression and/or function. In fact, modulation of alkaline phosphatase activity by sodium butyrate is known to be a marker for epithelial differentiation in the small intestine in vitro.[26] Furthermore, induction of expression of MUC3 and lysozyme (proteins involved in innate immunity and host defense) in epithelial cells[2] may be an epithelial-cell response to an enhanced burden of bacteria in the ileal pouch. Thus, intestinal adaptation appears to be a cooperative process involving phenotypic changes in epithelial cells as well as alterations in the composition of bacterial species.

Although fecal microbiota are known to reflect accurately the luminal bacterial population of the distal digestive tract, some reports have suggested that mucosa-associated microbiota may play a more important pathogenic role in inflammatory bowel disease than fecal microbiota.[27-29] In this study, "fecal" microbiota were used because of the ease of sampling from healthy individuals and patients. Previous DNA-based approaches have reported a similarity index of approximately 85% between fecal microbiota and mucosa-associated microbiota,[28-30] where the mucosal compartment is believed to derive from luminal bacteria.[30] Thus, analysis of fecal microbiota can be a useful tool for extrapolating events that may be induced by mucosa-associated microbiota. In an investigation of mucosa-associated flora using 16S rRNA-based analysis of 2 patients with an ileal pouch, Falk et al[31] concluded that mucosal microbiota in the ileal pouch also changed with time during the first year.

Our data demonstrate clearly that "colonic transformation" events occur both in the host and in the enteric microbiotic community. The increase in nonculturable bacterial populations is one of the major changes in fecal microbiota during ileal pouch development and is likely to contribute to physiologic changes such as intestinal adaptation and pathologic responses including pouchitis.

REFERENCES

1. Utsunomiya J, Iwama T, Imajo M, Matsuo S, Sawai S, Yaegashi K, et al. Total colectomy, mucosal proctectomy, and ileoanal anastomosis. Dis Colon Rectum 1980;23:459-66.
2. Fukushima K, Haneda S, Takahashi K, Ogawa H, Watanabe K, Funayama Y, et al. Molecular analysis of colonic transformation in the ileum after total colectomy in rats. Surgery 2006; 140:93-9.
3. Luckey TD. Introduction to intestinal microecology. Am J Clin Nutr 1972;25:1292-4.
4. Holzapfel WH, Haberer P, Snel J, Schillinger U, Huis in't Veld JH. Overview of gut flora and probiotics. Int J Food Microbiol 1998;41:85-101.
5. Ogawa H, Fukushima K, Sasaki I, Matsuno S. Identification of genes involved in mucosal defense and inflammation associated with normal enteric bacteria. Am J Physiol Gastrointest Liver Physiol 2000;279:G492-9.
6. Fukushima K, Ogawa H, Takahashi K, Naito H, Funayama Y, Kitayama T, et al. Non-pathogenic bacteria modulate colonic epithelial gene expression in germ-free mice. Scand J Gastroenterol 2003;38:626-34.
7. Nasmyth DG, Godwin PG, Dixon MF, Williams NS, Johnston D. Ileal ecology after pouch-anal anastomosis or ileostomy. A study of mucosal morphology, fecal bacteriology, fecal

volatile fatty acids, and their interrelationship. Gastroenterology 1989;96:817-24.
8. Smith FM, Coffey JC, Kell MR, O'Sullivan M, Redmond HP, Kirwan WO. A characterization of anaerobic colonization and associated mucosal adaptations in the undiseased ileal pouch. Colorectal Dis 2005;7:563-70.
9. Hayashi H, Sakamoto M, Benno Y. Phylogenetic analysis of the human gut microbiota using 16S rDNA clone libraries and strictly anaerobic culture-based methods. Microbiol Immunol 2002;46:535-48.
10. Langendijk PS, Schut F, Jansen GJ, Raangs GC, Kamphuis GR, Wilkinson MH, et al. Quantitative fluorescence in situ hybridization of *Bifidobacterium spp.* with genus-specific 16S rRNA-targeted probes and its application in fecal samples. Appl Environ Microbiol 1995;61:3069-75.
11. Hayashi H, Sakamoto M, Kitahara M, Benno Y. Molecular analysis of fecal microbiota in elderly individuals using 16S rDNA library and T-RFLP. Microbiol Immunol 2003; 47:557-70.
12. Sakamoto M, Hayashi H, Benno Y. Terminal restriction fragment length polymorphism analysis for human fecal microbiota and its application for analysis of complex bifidobacterial communities. Microbiol Immunol 2003;47:133-42.
13. Sakamoto M, Takeuchi Y, Umeda M, Ishikawa I, Benno Y. Application of terminal RFLP analysis to characterize oral bacterial flora in saliva of healthy subjects and patients with periodontitis. J Med Microbiol 2003;52:79-89.
14. Hayashi H, Takahashi R, Nishi T, Sakamoto M, Benno Y. Molecular analysis of jejunal, ileal, caecal and recto-sigmoidal human colonic microbiota using 16S rRNA gene libraries and terminal restriction fragment length polymorphism. J Med Microbiol 2005;54:1093-101.
15. Moyer CL, Tiedje JM, Dobbs FC, Karl DM. A computer-simulated restriction fragment length polymorphism analysis of bacterial small-subunit rRNA genes: efficacy of selected tetrameric restriction enzymes for studies of microbial diversity in nature. Appl Environ Microbiol 1996;62: 2501-7.
16. Marsh TL, Saxman P, Cole J, Tiedje J. Terminal restriction fragment length polymorphism analysis program, a web-based research tool for microbial community analysis. Appl Environ Microbiol 2000;66:3616-20.
17. Matsumoto M, Sakamoto M, Hayashi H, Benno Y. Novel phylogenetic assignment database for terminal-restriction fragment length polymorphism analysis of human colonic microbiota. J Microbiol Methods 2005;61:305-19.
18. Farrelly V, Rainey FA, Stackebrandt E. Effect of genome size and rrn gene copy number on PCR amplification of 16S rRNA genes from a mixture of bacterial species. Appl Environ Microbiol 1995;61:2798-801.
19. Hiraishi A, Iwasaki M, Shinjo H. Terminal restriction pattern analysis of 16S rRNA genes for the characterization of bacterial communities of activated sludge. J Biosci Bioeng 2000;90:148-56.
20. Matsuki T, Watanabe K, Fujimoto J, Takada T, Tanaka R. Use of 16S rRNA gene-targeted group-specific primers for real-time PCR analysis of predominant bacteria in human feces. Appl Environ Microbiol 2004;70:7220-8.
21. Collins MD, Lawson PA, Willems A, Cordoba JJ, Fernandez-Garayzabal J, Garcia P, et al. The phylogeny of the genus Clostridium: proposal of five new genera and eleven new species combinations. Int J Syst Bacteriol 1994;44:812-26.
22. Collado MC, Calabuig M, Sanz Y. Differences between the fecal microbiota of coeliac infants and healthy controls. Curr Issues Intest Microbiol 2007;8:9-14.
23. Kleessen B, Kroesen AJ, Buhr HJ, Blaut M. Mucosal and invading bacteria in patients with inflammatory bowel disease compared with controls. Scand J Gastroenterol 2002;37: 1034-41.
24. Barcenilla A, Pryde SE, Martin JC, Duncan SH, Stewart CS, Henderson C, et al. Phylogenetic relationships of butyrate-producing bacteria from the human gut. Appl Environ Microbiol 2000;66:1654-61.
25. Hove H, Mortensen PB. Short-chain fatty acids in the non-adapted and adapted pelvic ileal pouch. Scand J Gastroenterol 1996;31:568-74.
26. Fukushima K, Sasaki I, Hasegawa H, Takahashi K, Naito H, Funayama Y, et al. Sodium butyrate-induced liver-type alkaline phosphatase activity in a small intestinal epithelial cell line, IEC6. Dig Dis Sci 1998;43:1116-23.
27. Swidsinski A, Ladhoff A, Pernthaler A, Swidsinski S, Loening-Baucke V, Ortner M, et al. Mucosal flora in inflammatory bowel disease. Gastroenterology 2002;122:44-54.
28. Marteau P, Lepage P, Mangin I, Suau A, Dore J, Pochart P, et al. Review article: gut flora and inflammatory bowel disease. Aliment Pharmacol Ther 2004;20(Suppl 4):18-23.
29. Lepage P, Seksik P, Sutren M, de la Cochetiere MF, Jian R, Marteau P, et al. Biodiversity of the mucosa-associated microbiota is stable along the distal digestive tract in healthy individuals and patients with IBD. Inflamm Bowel Dis 2005;11:473-80.
30. Sokol H, Seksik P, Rigottier-Gois L, Lay C, Lepage P, Podglajen I, et al. Specificities of the fecal microbiota in inflammatory bowel disease. Inflamm Bowel Dis 2006;12: 106-11.
31. Falk A, Olsson C, Ahrne S, Molin G, Adawi D, Jeppsson B. Ileal pelvic pouch microbiota from two former ulcerative colitis patients, analysed by DNA-based methods, were unstable over time and showed the presence of Clostridium perfringens. Scand J Gastroenterol 2007;42:973-85.